Modelo computacional del proceso de remodelado óseo en la sutura sagital

Francisco Javier Burgos Flórez

Universidad Nacional de Colombia

Facultad de Medicina

Bogotá, Colombia

Diciembre de 2015

Modelo computacional del proceso de remodelado óseo en la sutura sagital

Francisco Javier Burgos Flórez

Trabajo de investigación presentado como requisito parcial para optar al título de:

Magister en Ingeniería Biomédica

Director:

Diego Alexander Garzón Alvarado, Ph.D.

Línea de Investigación:

Mecanobiología de órganos y tejidos

Grupo de Investigación:

Grupo de Modelado y Métodos Numéricos GNUM

Grupo de Mecanobiología de Tejidos y Órganos

Universidad Nacional de Colombia

Facultad de Medicina

Bogotá, Colombia

Diciembre de 2015

Este trabajo se lo dedico

A mi madre, por todo el amor y apoyo incondicional que me ha dado.

A mi tía María Stella (Tita), mi segunda madre, por apoyarme y estar para mí en los momentos difíciles de mi vida.

A Roxana, mi amor, mi amiga, la mujer de mi vida.

Agradecimientos

La realización de este trabajo ha significado un gran avance en mi desarrollo profesional y personal. Por ello, quisiera agradecer a todas las personas que de una u otra forma aportaron hacia la culminación del mismo.

A mi director Diego Alexander Garzón Alvarado, Ph.D., por orientarme a lo largo de estos años y brindarme la oportunidad de aplicar la ingeniería en problemas de la medicina y la biología en su grupo de investigación. Le agradezco por brindarme su conocimiento, apoyo, palabras de aliento, gran dedicación y ayudarme a crecer tanto profesional como personalmente.

Al profesor Eduardo Romero, Ph.D, por brindarme sus valiosos conocimientos en metodología de investigación.

A las profesoras Afife Mrad De Osorio y Yoshie Adriana Hata Uribe, por guiarme a lo largo de este trabajo y brindarme sus conocimientos en biología y experimentación animal.

A Johana Guevara, por su continua disponibilidad para ayudarme y orientarme en mi investigación. Gracias por tus consejos, correcciones y continua asesoría.

A Miguel Moncayo, por brindarme su apoyo y conocimientos en biología.

A Aura Forero, por su apoyo y amistad durante estos años.

A Rosy, Alejandra, Juan, Héctor y Yaneth, por asesorarme y brindarme su conocimiento a lo largo de estos años.

Por último, pero no menos importante, le agradezco mucho a mi tía Marujita por acogerme en Bogotá al inicio de mis estudios de maestría. Gracias por darme tu amistad y cariño incondicional.

Resumen

Los procesos de formación y crecimiento de huesos planos y formación e interdigitación de suturas de la calota humana están controlados por una compleja interacción entre factores genéticos, bioquímicos y medioambientales que regulan la síntesis y reabsorción de hueso durante el desarrollo prenatal y la infancia. A pesar de que diversos estudios han demostrado experimentalmente el rol de los principales factores bioquímicos en estos procesos, aún no se conocen los mecanismos subyacentes que los controlan. Por lo tanto, este trabajo propone un modelo matemático de los procesos de formación de huesos planos y suturas, tomando en cuenta varios eventos biológicos. Inicialmente, se modela el crecimiento de los huesos planos y la formación de suturas y fontanelas como un sistema de reacción difusión entre dos proteínas: TGF-β2 y TGF-β3. La primera es expresada por osteoblastos y permite la diferenciación de células mesenquimales adyacentes en los frentes de los huesos planos. La segunda es expresada por células mesenquimales en las suturas e inhibe su diferenciación hacia osteoblastos en los frentes de los huesos. La interdigitación de las suturas es modelada utilizando un sistema de ecuaciones de reacción difusión que genera patrones espacio-temporales de formación y reabsorción de huesos mediante dos moléculas (Wnt y Esclerostina), las cuales controlan la diferenciación de células mesenquimales a osteoblastos en estos sitios. Los resultados de las simulaciones predicen el crecimiento de los huesos planos a partir de centros de osificación, la formación de suturas y fontanelas, y la generación de eventos de formación y reabsorción de hueso que dan lugar a los patrones interdigitados. Estas etapas fueron modeladas y resueltas mediante el método de los elementos finitos. Los resultados de la simulación coinciden con las características morfológicas de los huesos planos y suturas de la calota durante el desarrollo prenatal y la infancia humana.

Palabras clave: Ecuaciones de reacción-difusión, osificación intramembranosa, remodelado óseo, método de los elementos finitos, craneosinostosis.

Abstract

The processes of flat bones growth, sutures formation and interdigitation in the human calvaria are controlled by a complex interaction between genetic, biochemical and environmental factors that regulate bone formation and resorption during prenatal development and infancy. Despite previous experimental evidence accounting for the role of the main biochemical factors acting on these processes, the underlying mechanisms controlling them are still unknown. Therefore, we propose a mathematical model of the processes of flat bone and suture formation, taking into account several biological events. First, we model the growth of the flat bones and the formation of sutures and fontanels as a reaction diffusion system between two proteins: TGF-β2 and TGF-β3. The former is expressed by osteoblasts and allows adjacent mesenchymal cells differentiation on the bone fronts of each flat bone. The latter is expressed by mesenchymal cells at the sutures and inhibits their differentiation into osteoblasts at the bone fronts. Suture interdigitation is modelled using a system of reaction diffusion equations that develops spatio-temporal patterns of bone formation and resorption by means of two molecules (Wnt and Sclerostin) which control mesenchymal cells differentiation into osteoblasts at these sites. The results of the computer simulations predict flat bone growth from ossification centers, sutures and fontanels formation as well as bone formation and resorption events along the sutures, giving rise to interdigitated patterns. These stages were modelled and solved by the finite elements method. The simulation results agree with the morphological characteristics of calvarial bones and sutures throughout human prenatal development and infancy.

Keywords: Reaction-diffusion equations, intramembranous ossification, bone remodeling, finite elements method, craniosynostosis.

Contenido

Resumen ..... **IX**

Lista de figuras ..... **XIII**

Lista de tablas ..... **XV**

Introducción **17**

1. Flat bones and sutures formation in the human cranial vault during prenatal development and infancy: A computational model **19**

1.1 Introduction 19
1.2 Materials and methods 24
1.2.1 Hypotheses on the formation of flat bones and sutures of the human cranial vault 24
1.3 Model description 26
1.3.1 First event: Emergence of the primary ossification centers 26
1.3.2 Second event: Bone growth and suture formation 27
1.3.3 Third event: Suture interdigitation and fusion 32
1.4 Numerical implementation 35
1.4.1 Implementation of the second developmental stage 35
1.4.2 Implementation of the third developmental stage 36
1.4.3 Suture interdigitation in the 3d model 37
1.4.4 Parameters 39
1.5 Results 42
1.5.1 Second event: Bone growth and suture formation 42
1.5.2 Third event: Suture interdigitation and fusion 44
1.6 Discussion 48
1.7 Future Work 55
1.8 Conclusion 55

Appendix A. Estimation of the values of the parameters **57**

References **61**

Lista de figuras

PÁG.

FIGURE 1-1: (A) CORONAL VIEW OF THE NEONATAL CALVARIA. MODIFIED FROM [6]. (B) CORONAL VIEW OF AN ADULT CALVARIA WITH LAMBDOID AND SAGITTAL SUTURES SHOWING INTERDIGITATIONS. MODIFIED FROM [7]. 20
FIGURE 1-2: MOLECULAR AND CELLULAR PROCESSES INVOLVED IN THE STAGES OF FLAT BONE FORMATION AND GROWTH AND SUTURE FORMATION. SOLID LINES MEAN ACTIVATION, DASH LINES INHIBITION, DOTTED LINES INDICATE A SIGNAL TRANSDUCTION. 25
FIGURE 1-3: STAGES INVOLVED IN THE PROCESS OF SUTURE INTERDIGITATION AND FUSION. SOLID LINES MEAN ACTIVATION, DASH LINES INHIBITION. 26
FIGURE 1-4: SCHEMATIC SHOWING THE PROCESSES OF FLAT BONE GROWTH AND SUTURE FORMATION MEDIATED BY TGF-B2 AND TGF-B3 CONCENTRATIONS. OSTEOBLAST LOCATED ON THE BONE FRONTS EXPRESS TGF-B2 (DOTTED BLUE ARROWS), WHILE MESENCHYMAL CELLS AT THE SUTURES EXPRESS TGF-B3 (DOTTED BROWN ARROWS). ADJACENT MESENCHYMAL CELLS DIFFERENTIATION IS ASSUMED AS DEPENDENT OF THE CONCENTRATION OF BOTH MOLECULES, WHERE TGF-B2 PROMOTES THEIR DIFFERENTIATION (CONTINUOUS BLUE ARROWS) AND TGF-B3 INHIBITS IT (CONTINUOUS BROWN ARROWS). THE TIME EVOLUTION OF TGF-B3 AND TGF-B2 CONCENTRATIONS ALLOWS THE GROWTH OF THE FLAT BONES AND THE FORMATION OF THE SUTURES DURING PRENATAL DEVELOPMENT. 31
FIGURE 1-5: SCHEMATIC SHOWING THE PROCESS OF SUTURE INTERDIGITATION IN A BI-DIMENSIONAL SEGMENT OF A BONE-SUTURE-BONE INTERFACE. (A) ASSUMED INITIAL PATTERN OF BONE FORMATION DRIVEN BY LOCATIONS OF HIGH WNT CONCENTRATION (BONE IN LIGHT YELLOW, SUTURE IN LIGHT PINK). (B) RESULTING PATTERN OF BONE RESORPTION. WE CAN SEE HOW BONE FORMATION PATTERNS ON ONE BONE FRONT ARE REFLECTED ON THE OPPOSING FRONT AS RESORPTION SITES, AS SHOWN WITH BLUE ARROWS. NEW SITES OF SUTURE GROWTH ARE DISPLAYED IN DARK PINK. (C) SUTURE PATTERN OBTAINED FROM BONE FORMATION AND RESORPTION EVENTS. (D) RESULTING PATTERN OF SUTURE INTERDIGITATION AFTER CONSIDERING THE REDUCTION IN SUTURE WIDTH PRODUCED BY BONE FORMATION EVENTS REGULATED BY TGF-B2 AND TGF-B3 CONCENTRATIONS. (BONE IN LIGHT YELLOW, SUTURE IN LIGHT PINK). 34
FIGURE 1-6: (A) PRENATAL SKULL, (B) SIMPLIFIED GEOMETRY WITH 8353 NODES AND 16549 TRIANGULAR ELEMENTS. (C) AND (D). GEOMETRIC RELATIONSHIPS USED IN THE COMPUTATIONAL MODEL. A = 32 MM, B = 48 MM (B/A = 1.5), C = 16 MM, D = 9.6 MM AND R = 8 MM. 37
FIGURE 1-7: (A) CORONAL VIEW OF THE NEONATAL CALVARIA. ADAPTED FROM [56]. (B) SEGMENT OF THE SAGITTAL SUTURE CONSIDERED. (C) BI-DIMENSIONAL MESH WITH 15140 NODES AND 29822 TRIANGULAR ELEMENTS. 39
FIGURE 1-8: TIME EVOLUTION OF THE TGF-B2 CONCENTRATION FOR THE FRONTAL BONES DURING PRENATAL DEVELOPMENT. THE AREAS OF INITIAL RELEASE OF TGF-B2 CORRESPOND TO THE PRIMARY OSSIFICATION CENTERS. (A) RIGHT FRONTAL BONE. (B) LEFT FRONTAL BONE. TIME (T) IS EXPRESSED IN MONTHS (M). 42

FIGURE 1-9: TGF-B3 CONCENTRATION AND BONE FORMATION DURING NORMAL PRENATAL DEVELOPMENT. (A) TIME EVOLUTION OF TGF-B3. AREAS OF HIGH TGF-B3 CONCENTRATION DEFINED THE SITES OF SUTURE FORMATION. (B) TIME EVOLUTION OF BONE FORMATION OF THE FLAT BONES DURING PRENATAL DEVELOPMENT. FLAT BONES GROW RADIALLY FOLLOWING THE DIFFUSION OF THE MOLECULE TGF-B2 AND THEIR GROWTH DIMINISHES DUE TO THE EXPRESSION OF TGF-B3 BY THE MESENCHYMAL CELLS AT THE SUTURES SITES. THE BONES LEAVE WIDE SPACES BETWEEN THEM, CALLED FONTANELS AND SUTURES, WHICH COINCIDE WITH AREAS WITH TGFB-3 CONCENTRATIONS HIGHER THAN 0.6 NG/ML. THEREFORE, PREMATURE SUTURE OSSIFICATION IS INHIBIT. TIME (T) IS EXPRESSED IN MONTHS (M). 43

FIGURE 1-10: RESULTS OF TGF-B3 CONCENTRATION AND BONE FORMATION AT THE METOPIC SUTURE FOR DIFFERENT VALUES OF THE CONSTANT $\boldsymbol{\gamma 4}$ IN EQUATION (1-2) FOR TIME T=3.5 MONTHS PRENATAL. (A) TGF-B3 CONCENTRATION IN THE METOPIC SUTURE. (B) BONE FORMATION IN THE METOPIC SUTURE. NOTE HOW THE INCREMENT OF $\boldsymbol{\gamma 4}$ REGULATES BONE FORMATION AT THE SITE OF THE METOPIC SUTURE, GOING FROM PREMATURE FUSION TO PATENCY. UNITS OF $\boldsymbol{\gamma 4}$ ARE IN $\boldsymbol{10 - 8ml2cel.s.ng}$. 44

FIGURE 1-11: STEADY STATE RESPONSE OF THE CONCENTRATION OF WNT AND SCLEROSTIN FOR A BI-DIMENSIONAL SEGMENT OF THE SAGITTAL SUTURE..... 45

FIGURE 1-12: RESULTS OF PROCESS OF SUTURE INTERDIGITATION DURING INFANCY FOR A BI-DIMENSIONAL SEGMENT OF THE SAGITTAL SUTURE. NOTE THE BEGINNING OF INTERDIGITATION AT 12 MONTHS OF AGE AND THE CONTINUOUS NARROWING OF THE SUTURE THROUGHOUT INFANCY. SUTURE IS DEPICTED IN BLACK, BONE IN WHITE. TIME (T) IS EXPRESSED IN MONTHS (M). 45

FIGURE 1-13: TIME EVOLUTION OF THE PROCESS OF SUTURE INTERDIGITATION AND FUSION DURING POSTNATAL DEVELOPMENT FOR THE CORONAL AND SAGITTAL SUTURES. TIME (T) IS EXPRESSED IN MONTHS (M). 46

FIGURE 1-14: TIME EVOLUTION OF THE PROCESS OF SUTURE INTERDIGITATION AND FUSION DURING POSTNATAL DEVELOPMENT FOR THE LAMBDOID AND SAGITTAL SUTURES. TIME (T) IS EXPRESSED IN MONTHS (M). 47

FIGURE 1-15: MORPHOLOGICAL COMPARISON BETWEEN SIMULATION RESULTS AND ADULT CALVARIA. (A) SIMULATION RESULTS FOR SUTURE INTERDIGITATION AND FUSION DURING INFANCY. (B) ADULT CALVARIA. 48

FIGURE 1-16: RESULTS COMPARISON BETWEEN DIFFERENT COMPUTATIONAL STUDIES. A) RESULTS FOR BONE FORMATION IN THE CRANIAL VAULT IN THE MOUSE [36]. WE CAN SEE THE FORMATION OF EACH FLAT BONE AS WELL AS THE FORMATION OF FONTANELS. B) BONE FORMATION IN THE HUMAN CRANIAL VAULT OF OUR PREVIOUS COMPUTATIONAL STUDY [34], WHICH CONSIDERS BONE GROWTH MEDIATED BY TRANSCRIPTION FACTOR DLX5. C) RESULTS OF BONE AND SUTURE FORMATION IN THIS WORK. D) PICTORIAL VIEW OF THE REAL HUMAN CRANIAL VAULT AFTER BIRTH. NOTE THE MORPHOLOGICAL SIMILARITIES BETWEEN THE RESULTS FROM THIS WORK AND THE REAL CALVARIA IN TERMS OF FLAT BONES AND SUTURES LOCATION AND MORPHOLOGY. 51

Lista de tablas

PÁG.

TABLE 1-1: PARAMETERS USED IN THE MODEL. 39
TABLE 1-2: CONNECTION BETWEEN THE NON-DIMENSIONAL SCHNAKENBERG MODEL AND THE VIBRATION MODES ACCORDING TO THE PARAMETERS OBTAINED IN THE LINEAR ANALYSIS. 59

Introducción

Los procesos de formación y crecimiento de huesos planos y formación e interdigitación de suturas de la calota humana están controlados por una compleja interacción entre factores genéticos, bioquímicos y medioambientales que regulan la síntesis y reabsorción de hueso durante el desarrollo prenatal y la infancia. La existencia de alteraciones en estos procesos está relacionada con la aparición de patologías como la craneosinostosis, condición caracterizada por una fusión prematura de las suturas de la calota, la cual genera alteraciones morfológicas del cráneo y retardos en el desarrollo cognitivo. A pesar de que diversos estudios han demostrado experimentalmente el rol de los principales factores bioquímicos y genéticos presentes durante la morfogénesis de huesos y suturas de la calota, aún no existe un consenso en cuanto a los procesos biológicos que dan lugar a la formación de estos tejidos y, en particular, cuáles son los mecanismos biológicos subyacentes que dan lugar a la formación, mantenimiento e interdigitación de las suturas. Adicionalmente, la dificultad intrínseca de la experimentación in vivo ha obstaculizado la cuantificación de los efectos de estos factores y como su interacción regula la formación de hueso en la calota. Por lo tanto, este trabajo propone un modelo matemático con enfoque bioquímico de los procesos de formación de los huesos planos y suturas de la calota, fundamentado en las ecuaciones de reacción difusión, el cual es implementado computacionalmente mediante el método de los elementos finitos. La simulación del modelo predice la formación y crecimiento de los huesos planos a partir de centros de osificación primarios, la formación de las suturas y fontanelas al final de la etapa embrionaria y la evolución espacio-temporal de los procesos de síntesis y reabsorción ósea que generan patrones de osificación interdigitados a lo largo de las suturas durante la infancia. Los resultados obtenidos sugieren que la fusión prematura de las suturas puede ser el resultado de alteraciones en la habilidad de las células de las suturas de expresar proteínas osteo-inhibitorias en respuesta a señales bioquímicas osteo-inductivas provenientes de los frentes de osificación de los huesos planos, mientras que la posterior interdigitación puede ser explicada por procesos acoplados de formación y reabsorción de hueso controlados por la expresión de proteínas osteo-inductivas y osteo-inhibitorias a lo

largo de las suturas. Por lo anterior, este trabajo ofrece una herramienta teórica para el estudio de la morfogénesis de huesos planos y suturas así como patologías relacionadas como la craneosinostosis, generando de esta forma una mayor compresión de los mecanismos reguladores del desarrollo craneal humano.

La realización de este trabajo tuvo como resultado la publicación de un artículo científico en la revista científica “Journal of Theoretical Biology”. Por lo tanto, el capítulo 1 de este documento presenta el artículo publicado.

1. Flat bones and sutures formation in the human cranial vault during prenatal development and infancy: A computational model

This chapter was published as a scientific paper in the Journal of Theoretical Biology (Impact Factor: 2.116): Burgos-Flórez FJ, Gavilán-Alfonso ME, Garzón-Alvarado DA. Flat bones and sutures formation in the human cranial vault during prenatal development and infancy: A computational model. Journal of Theoretical Biology 2016; 393:127-144. The paper can be found online at: http://dx.doi.org/10.1016/j.jtbi.2016.01.006.

1.1 Introduction

The flat bones that make up the human cranial vault (frontal, parietal, temporal and occipital) begin their formation between eighth and ninth week of gestation, growing from ossification centers through intramembranous ossification [1]. In this process, mesenchymal cells located inside the fibrous connective tissue membrane, covering the brain, proliferate and differentiate into osteoblasts, which synthesize osteoid, the organic portion of bone. Mineralization of osteoid will result in new bone tissue [2]. The continuous growth of the flat bones of the calvaria ensures a normal morphology of the head and allows a rapid expansion of the brain [3], which increases its size at high speed during embryonic development and reaches 80% of its final volume in adulthood after two years of life [3].

At the end of the embryonic stage, the ossification fronts of the flat bones of the calvaria are separated by non-ossified tissue barriers, known as sutures and fontanels (see **Fig. 1-1a**). The former are joints composed by bands of fibrous connective tissue that unite the ossifications fronts of the flat bones, and include: coronal sutures (space between the two frontal and parietal bones), lambdoid sutures (between the two parietal and the occipital

bones), metopic sutures (between the frontal bones) and sagittal sutures (between the parietal bones) [4]. In addition, the sutures serve as the main sites of bone formation in the skull [4]. Therefore, the overall shape of it is determined by the processes of bone formation along the suture margins [5]. Fontanels are membranous sites in the developing cranial vault that haven't ossified yet and work as high deformation areas where the brain can expand. They consist of the anterior fontanel (diamond-shape space located between the two frontal and two parietal bones at the junction of the coronal, sagittal and metopic suture) and the posterior fontanel (triangle-shaped space between the two parietal bones and the occipital bone at the junction of the sagittal and lambdoid suture).

Figure 1-1: (a) Coronal view of the neonatal calvaria. Modified from [6]. (b) Coronal view of an adult calvaria with lambdoid and sagittal sutures showing interdigitations. Modified from [7].

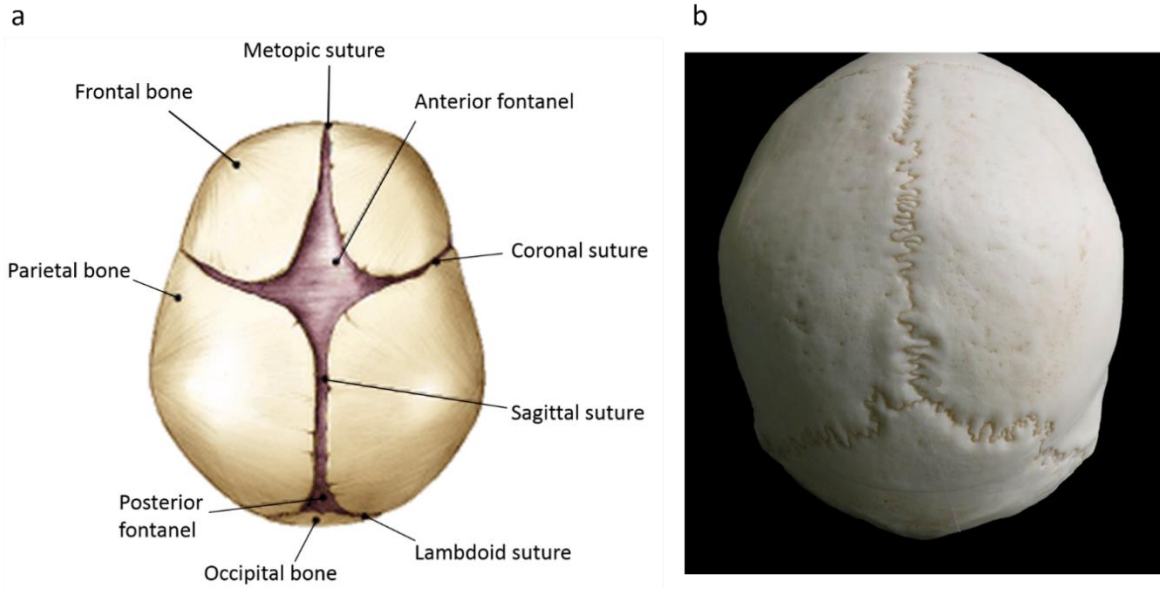

As postnatal development progresses, the cranial sutures exhibit morphological changes, going from straight lines to an interdigitated pattern, with a corresponding increase in suture length [8] (see **Fig. 1-1b**). It is considered that interdigitation arises from a continuous interplay between bone formation and resorption events taking place at the sutures convexities and concavities, respectively [9]. The bone formation processes, at the bone fronts of the flat bones, progressively decrease the width of the sutures, until these fully

ossify. For the metopic suture, suture fusion is usually completed before nine months of age [10], while coronal, sagittal and lambdoid sutures will fuse around the third decade of life [11].

Numerous studies have focused on determining the mechanisms underlying the processes of bone growth and suture formation and interdigitation. In general, it is believed that a complex interaction among different genetic, biochemical and environmental factors exists, where local spatio-temporal variations in both cellular signaling and mechanotransduction mechanisms might play a crucial role [5,12–17]. Several *in vitro* and *in vivo* studies have tried to establish the role of the main molecular factors acting during these developmental processes. Amongst them, regional variations in the concentrations of transforming growth factor beta three (TGF-β3) and transforming growth factor beta two (TGF-β2) have been found between patent and prematurely fused sutures [18–22], implying an osteoinhibitory role for TGF-β3 and an osteoinductive role for TGF-β2 during suture formation and maintenance. These findings are in concordance with a previous hypothesis from Opperman et al. [17], which suggest that suture phenotypic maintenance is dependent on the spatial concentrations of both osteogenic inhibitors and promoters coming from the endocranium, a membrane which is part of the dura mater and is in contact with the skull. The subsequent interdigitation of sutures during infancy has been related to linked bone formation and resorption events along their length controlled by osteoblast and osteoclast function [9]. Recently, the Wnt family of glycoproteins, expressed predominantly by osteocytes, have been associated to bone homeostasis, where its canonical pathway, the Wnt/β-catenin signaling pathway, has been experimentally shown to regulate mesenchymal cells differentiation into osteoblasts at the bone fronts [23–25]. On the other hand, Sclerostin, a protein also secreted by osteocytes, have been shown to inhibit bone formation by antagonizing the Wnt/β-catenin signaling pathway [26–28]. In turn, resorption events have been associated with the concentration of receptor activator of nuclear factor kappa-B ligand (RANKL), a protein required for osteoclast differentiation, shown to be expressed by both osteocytes alone and active osteoblasts through the Wnt/β-catenin signaling pathway [29–33].

However, despite previous experimental evidence accounting for the role of different biochemical factors on the processes of suture formation and interdigitation, the underlying

biological mechanisms controlling these processes are still unknown. Additionally, the intrinsic difficulty of live experimentation has hindered the quantification of the way these molecules interact and regulate bone growth along the calvaria. Hence, no consensus exists about the ways sutures are formed during prenatal development and change their morphology during infancy.

As a result, the use of computational techniques has emerged as an alternative to conventional experimentation, resulting in the development of mathematical models and computer simulations focused on establishing the biological mechanisms driving flat bone formation and suture formation and interdigitation. Using a biochemical framework, Garzón-Alvarado et al. [34,35] formulated a computational model of the process of flat bone formation and growth during embryonic development using a system of reaction diffusion equations between BMP2 and Noggin. The model simulated the appearance of the primary ossification centers of each of the cranial bones, which were regulated by spatio-temporal patterns developed from a Turing instability of the system. They also modelled mesenchymal cells differentiation into osteoblasts using Dxl5, a transcription factor related to the regulation of differentiation of mesenchymal cells at the osteogenic fronts of each flat bone of the calvaria [17]. They could predict the growth of the skull bones and the formation of the fontanels during embryonic development. Lee et al. [36] developed a computational model of bone formation in the mouse cranial vault. They predicted the relative locations of five ossification centers and simulated the growth of the mouse flat bones. Khonsari RH et al. [37] developed a mathematical model of the onset of suture interdigitation applying quasi-static tensile loads on the sagittal suture during early postnatal development. The model predicted the onset of interdigitations in sutures and the alignment of collagen fibers with the direction of the considered traction loads. Miura et al. [38] simulated the onset of interdigitation evidenced in the cranial sutures during the first year after birth. They modeled the process from a biological point of view, proposing a system of reaction diffusion equations between two types of molecules: bone growth inhibitory factors such as Noggin and osteoinductive proteins like the fibroblast growth factors (FGFs). The model could predict the maintenance of the sutures during the first months after birth and its modification towards an interdigitated pattern. Zollikofer et al. [39] proposed a model of suture formation using the Laplace equation. They simulated a variety of sutural forms, concluding that strain

and morphogen sensitivity of the sutures, as well as its viscosity, might be key factors in suture complexity.

Although the described mathematical models have increased our understanding of flat bone and suture morphogenesis, these models did not consider the mechanisms by which sutures form and remain unossified in the presence of radial flat bone growth during prenatal development. Similarly, a clear explanation about the mechanisms driving suture interdigitation is still missing, since previous computational studies have only accounted for the role of bone formation processes along the sutures, leaving aside the role of bone resorption processes on the onset of the interdigitated patterns. Considering that biochemical factors control bone formation and resorption processes through their spatio-temporal concentrations, there is no quantification of their effects on bone morphogenesis along the calvaria throughout prenatal development and infancy. Thus, a better understanding of the expression of these molecules, along with the timing of expression, may provide an opportunity for future targeted genetic therapies for the treatment of pathologies associated with calvarial morphogenesis [40].

Therefore, the aim of this paper is to provide a novel explanation about the mechanism underlying suture formation and interdigitation and how the spatio-temporal concentrations of different biochemical factors regulate bone formation and resorption processes along the calvaria, giving rise to radial bone growth from ossification centers during prenatal development, suture formation at late stages of prenatal development and suture interdigitation during infancy. To do this, we follow the formulation made by Garzón-Alvarado et al. [34,35] regarding flat bone formation from primary ossification centers, with a focus on modeling the processes of suture formation and interdigitation using a purely biochemical scheme based on reaction diffusion equations. Our approach considers the effects of the concentrations of TGF-β3, TGF-β2, Wnt and Sclerostin, proteins widely studied in reported experimental studies, on flat bone and suture morphogenesis during prenatal development and infancy, by modeling and simulating the following biological processes:

- The growth of the flat bones of the calvaria during prenatal development.

- The formation and maintenance of the lambdoid, coronal, metopic and sagittal sutures and the formation of the anterior and posterior fontanels during prenatal development.
- The interdigitation of the coronal, lambdoid and sagittal sutures, and the fusion of the metopic suture during infancy.

The simulation results agree with the morphological characteristics of flat bones and sutures of the calvaria throughout human prenatal development and infancy. This work is, to our knowledge, the first attempt to develop a mathematical framework that describes the processes regulating bone and suture formation during human calvarial development.

1.2 Materials and methods

1.2.1 Hypotheses on the formation of flat bones and sutures of the human cranial vault

This article assumes that the processes of flat bone formation and suture formation and interdigitation are regulated by three consecutive events: The formation (First event) of flat bones is controlled by the differentiation of mesenchymal cells into osteoblasts regulated by the spatio-temporal concentration of two molecules, BMP2 and Noggin. These molecules form a reaction diffusion system that develops spatial patterns, where high concentrations of BMP2 determine the regions where mesenchymal cells differentiation into osteoblasts will take place [41]. Hence, BMP2 and Noggin regulate the sites where the primary ossification center will appear, thus controlling tissue differentiation in the cranial vault (see **Fig. 1-2**). This event has been previously modelled and simulated in [35]. Once primary ossification centers have developed, the growth of the flat bones and the formation of the sutures (Second event) are regulated by the concentrations of TGF-β2 and TGF-β3. The former is expressed along the ossification fronts of each developing flat bone, promoting adjacent mesenchymal cells differentiation into osteoblasts at these sites. TGF-β3 diffuses from the sutures, inhibiting the differentiation of mesenchymal cells into osteoblasts at the bone fronts [21,22]. Accordingly, bone formation taking place at the suture margins is mediated by the concentrations of both TGF-β2 and TGF-β3 (see **Fig. 1-2**). After birth, suture interdigitation takes place. We model interdigitation as a system of

reaction diffusion equations that generate a localized pattern of Wnt and Sclerostin, where high concentrations of Wnt trigger mesenchymal cells differentiation into osteoblasts at these sites, while high concentrations of Sclerostin will inhibit this differentiation [25,42,43]. We assume that the processes of bone formation along the bone fronts are coupled to the bone resorption ones, maintaining a balance in bone remodeling. Hence, if one osteogenic front experiences bone formation at an specific location, bone resorption will take place on the opposing bone front, given by osteoclast acting on these sites [9]. This hypothesis is based on previous studies accounting the role of osteoblasts and osteocytes in signaling hematopoietic stem cells differentiation into osteoclast by the expression of RANKL [29–33] (see **Fig. 1-3**). Thus, osteoblasts forming on a region of a bone front induce bone resorption on the opposing bone front by promoting osteoclastogenesis through RANKL expression. The formation of a resorption cavity is thus achieved by osteoclast acting on these sites.

Figure 1-2: Molecular and cellular processes involved in the stages of flat bone formation and growth and suture formation. Solid lines mean activation, dash lines inhibition, dotted lines indicate a signal transduction.

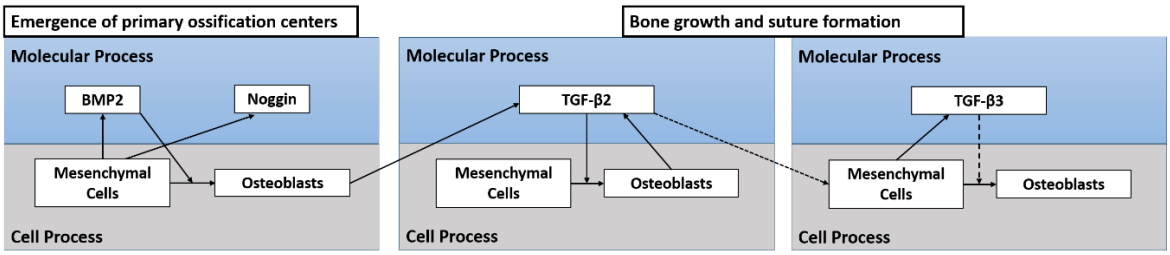

Figure 1-3: Stages involved in the process of suture interdigitation and fusion. Solid lines mean activation, dash lines inhibition.

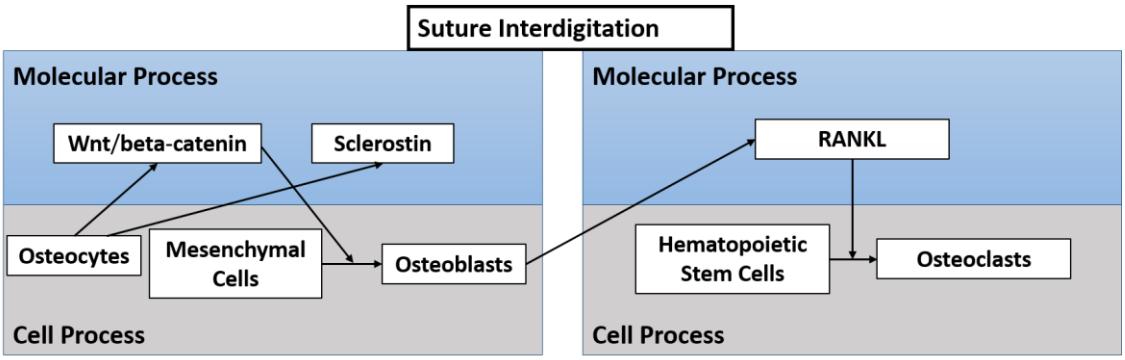

1.3 Model description

1.3.1 First event: Emergence of the primary ossification centers

Previous work [35] has focused on modelling the emergence of the primary ossification centers in the calvaria using a system of reaction diffusion equations between two molecules, BMP2 and Noggin. This system produces a diffusion driven instability, also known as Turing instability, where stable patters in time and unstable in space are obtained. It was proposed that regions of high BMP2 concentration will be the ones where mesenchymal cells differentiation into osteoblasts take place. In addition, this model took into account mesenchymal cells maturation, following the theory of Ruch et al. [44,45], which states that only those cells that have completed a prescribed number of cell cycles can differentiate to osteoblasts. Therefore, it is assumed that the cells position in the calvaria determines their differentiation due to cell cycles. In this way, mesenchymal cells differentiation into osteoblasts is dependent on cell maturation given by their spatial position in the calvaria and the concentration of BMP2 that signals the process. Accordingly, the biological events described in this paper follow the results obtained in [35] regarding the emergence of the primary ossification centers.

1.3.2 Second event: Bone growth and suture formation

The processes controlling flat bone formation and suture formation are still not well understood. Previous work has proposed that once primary ossification centers have emerged, further bone formation at the ossification fronts of each flat bone is achieved following the diffusion of the molecule DLX5 [34], a morphogen assumed to induce adjacent mesenchymal cells differentiation into osteoblasts at these sites, while also preventing fusion between growing flat bones. This hypothesis was based on reported experimental evidence suggesting that DLX5 is a transcription factor which induces osteoblasts differentiation and increases osteoblast's capacity to express bone differentiation markers and generate mineralized nodules [46]. Hence, DLX5 allows cells differentiation from within the cell and indirectly induces the differentiation of adjacent cells by the expression of differentiation markers. However, since DlX5 role lies inside the cell and hasn't been linked to suture formation and fusion, we suggest that these processes might be regulated by the action of other molecules located on the extracellular matrix, which diffuse throughout the calvaria and control these processes with a dependency on their spatial concentrations.
Therefore, this paper suggest that radial bone growth and suture formation might be better explained by the antagonist roles of diffusing molecules which induce and inhibit bone formation in the calvaria, such as the biochemical interaction between two growth factors, TGF-β2 and TGF-β3. These extracellular proteins have been experimentally shown to have opposite effects on bone formation processes along the calvaria, with TGF-β3 being determinant in the formation and maintenance of cranial sutures [19–22]. *In vitro* studies have shown that the addition of TGF-β2 and removal of TGF-β3 to fetal rat calvarial cultures induced suture fusion in normally patent sutures, while the addition of TGF-β3 prevented suture fusion in destined to fuse rat calvarial sutures [20,22]. Opperman et al. [21] suggest that these antagonistic roles are closely related to these molecules sharing the same surface receptor: Transforming growth factor beta receptor type 1 (TGF-βR-1). Since TGF-β3 is a more potent competitor than TGF-β2, it binds more rapidly than TGF-β2 to TGF-βR-1, while also down-regulating TGF-βR-1 expression. Hence, it reduces the ability of cells to respond to TGF-β2, a promoter of mesenchymal cells differentiation into osteoblasts [21].

Following these experimental evidence, we suggest that bone growth and suture formation depend on the osteoinductive role of TGF-β2 and the osteoinhibitory role of TGF-β3, given

by the evolution of their spatial concentrations during prenatal development. Thus, once primary ossification centers have emerged, osteoblasts located at the developing bone fronts release TGF-β2-be (TGF-β2 for each specific bone). This protein diffuses at the bone margins to allow adjacent differentiation of nearby mesenchymal cells into osteoblasts. The evolution of TGF-β2 concentration is formulated following the mathematical model for DLX5 diffusion given by [34]:

$$\frac{\partial S_{D-i}}{\partial t} = \alpha_p + \alpha_d + \alpha_t \tag{1-1}$$

where S_{D-i} is the concentration of TGF-β2 that depends on each ith bone, being i = (1) left parietal, (2) right parietal, (3) left frontal, (4) right frontal and (5) occipital (derived from two bones which rapidly coalesce); α_i corresponds to the production, degradation and transport coefficients regulating TGF-β2 (S_{D-i}) concentration in time and space. The production coefficient is given by:

$$\alpha_p = \alpha C_O \frac{S_{TD-i}^n}{S_{D-i}^n + S_{TD-i}^n} \tag{1-2}$$

where α is a constant which quantifies TGF-β2 production by osteoblasts (C_O) present in each ith flat bone; S_{TD-i} is the saturation concentration of TGF-β2, after which, osteoblasts do not release this molecule and n is a constant.

In addition, the degradation and transport coefficients of Eq. (1-1) are given by:

$$\alpha_d = -\beta \frac{\ln(2)}{\tau_D} S_{D-i} \tag{1-3}$$

$$\alpha_t = D_{D-i} \nabla^2 S_{D-i} \tag{1-4}$$

where β quantifies the degradation process of the molecule; τ_D is the average time of degradation and D_{D-i} is the diffusion coefficient of each ith bone [34].

Suture formation is assumed to be regulated by an osteoinhibitory signal, TGF-β3, antagonizing TGF-β2 in bone formation processes. This protein is expressed by mesenchymal cells located in the calvarial sutures. We assume that the production of TGF-β3 is dependent on the concentration gradient of TGF-β2. Thus, mesenchymal cells expression of TGF-β3 starts once the concentration of TGF-β2 exceeds a given threshold value. In this manner, mesenchymal cells differentiation at the osteogenic fronts of each flat bone is regulated by the spatio-temporal concentrations of TGF-β2 and TGF-β3. This article assumes that the time evolution of the concentration of TGF-β3 is given by:

$$\frac{\partial S_G}{\partial t} = \alpha_p + \alpha_d + \alpha_t \tag{1-5}$$

where α_i corresponds to the production, degradation and transport coefficients regulating TGF-β3 (S_G) concentration in time and space. The production coefficient is given by:

$$\alpha_p = h(\bar{x})B(\bar{x})\gamma_i C_m S_{D-i} S_{D-j} \frac{S_{TG}^m}{S_G^m + S_{TG}^m} \tag{1-6}$$

where γ_i is a constant which quantifies TGF-β3 production by mesenchymal cells (C_m) located on the non-ossified tissue for each cranial suture, being i = (1) sagittal suture, (2) left coronal suture, (3) right coronal suture, (4) metopic suture, (5) left lambdoid suture and (6) right lambdoid suture; S_{TG} is the saturation concentration of TGF-β3, after which, mesenchymal cells do not release this molecule; and m is a constant. S_{D-i} and S_{D-j} correspond to the local TGF-β2 concentrations coming from the flat bones which are nearer to the domain point of analysis. As an example, for a domain point near the metopic suture, S_{D-i} and S_{D-j} will be the concentrations of TGF-β2 coming from the ossification fronts of the left and right frontal bones (S_{D-3},S_{D-4}). Therefore, S_{D-i} and S_{D-j} are the maximum values of TGF-β2 at the current time for the point of analysis considered between the five possible values of TGF-β2, since TGF-β2 spatio-temporal concentration is modelled as a unique reaction diffusion equation for each developing flat bone.

The function $h(\bar{x})$ controls the beginning of TGF-β3 production by mesenchymal cells located at the sutures, and is given by:

$$h(\bar{x}) = \begin{cases} 1 \; if \; M(\overline{S_D}) > \xi \\ 0 \; other \; case \end{cases} \quad (1\text{-}7)$$

where the function $M(\overline{S_D})$ returns the two highest values of S_D. As an example, at the location of the sagittal suture, the highest values of S_D correspond to TGF-β2 concentrations expressed by osteoblasts located on the bone fronts of the left and right parietal bones (S_{D-1} and S_{D-2}). That means that when both these values are higher than a TGF-β2 threshold concentration given by ξ, the function $h(\bar{x})$ will be equal to 1. In this manner, TGF-β3 expression by mesenchymal cells is triggered on sites where TGF-β2 concentrations coming from opposing bone fronts reach a value higher than ξ.

In addition, the degradation and transport coefficients of Eq. (1-5) are given by:

$$\alpha_d = -\kappa \frac{\ln(2)}{\tau_G} S_G \quad (1\text{-}8)$$

$$\alpha_{dif} = D_G \nabla^2 S_G \quad (1\text{-}9)$$

where κ quantifies the degradation process of the molecule; τ_G is the average time of degradation and D_G is the diffusion coefficient of TGF-β3.

We model the process of mesenchymal cells differentiation into osteoblasts as a function of the concentrations of TGF-β3 and the highest value of TGF-β2 on the point of analysis, given by:

$$C_O(\bar{x}, t) = \lambda(S_{D-im} - S_G) \quad (1\text{-}10)$$

where $C_O(\bar{x}, t)$ is the concentration of osteoblasts; λ is a constant that quantifies mesenchymal cells differentiation into osteoblasts and S_{D-im} refers to the highest of the five possible values of S_{D-i} (TGF-β2 concentration) coming from each growing flat bone in that location and on the current time of analysis, remembering that TGF-β2 spatio-temporal

concentration is modelled as five reaction diffusion equations, one for each developing flat bone.

Finally, bone formation at the bone fronts is modelled trough the $B(\bar{x})$ function, an activation function that signals tissue differentiation, and it is given by:

$$B(\bar{x}) = \begin{cases} 1 \; if \; C_O(\bar{x}, t) < C_{OT} \\ 0 \; other \; case \end{cases} \tag{1-11}$$

where C_{OT} is the threshold concentration of osteoblasts. Hence, we assume that bone formation processes take place on regions where osteoblasts concentration has surpassed C_{OT}. Therefore, the function $B(\bar{x})$ will be equal to 1 only in locations where the tissue remains membranous and ossification hasn't occurred. Additionally, TGF-β3 production by mesenchymal cells will take place only on membranous sites of the calvaria, as seen in Eq. (1-6). **Fig. 1-4** shows a schematic of the described process.

Figure 1-4: Schematic showing the processes of flat bone growth and suture formation mediated by TGF-β2 and TGF-β3 concentrations. Osteoblast located on the bone fronts express TGF-β2 (dotted blue arrows), while mesenchymal cells at the sutures express TGF-β3 (dotted brown arrows). Adjacent mesenchymal cells differentiation is assumed as dependent of the concentration of both molecules, where TGF-β2 promotes their differentiation (continuous blue arrows) and TGF-β3 inhibits it (continuous brown arrows).

The time evolution of TGF-β3 and TGF-β2 concentrations allows the growth of the flat bones and the formation of the sutures during prenatal development.

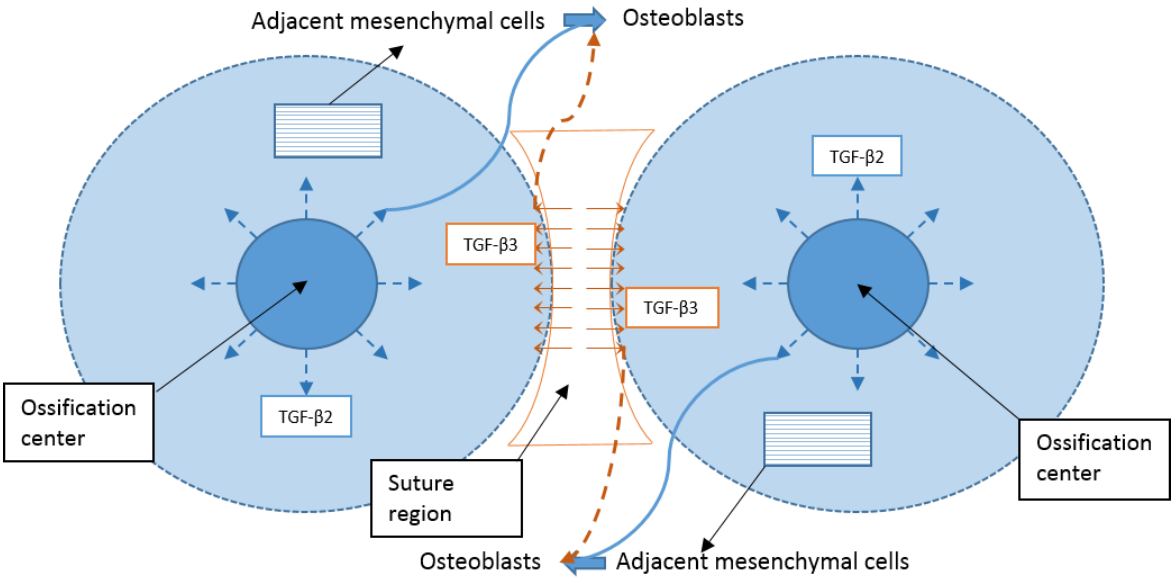

1.3.3 Third event: Suture interdigitation and fusion

The processes of suture interdigitation and fusion take place during postnatal development, once sutures and fontanels have been formed. These processes are assumed to be regulated by two molecules, Wnt and Sclerostin [23,26–28,49]. Both of them are expressed by osteocytes located near the bone fronts of each flat bone in the calvaria [23,28]. Wnt expression by osteocytes regulates the process of mesenchymal cells differentiation into osteoblasts at the sutures through the Wnt/β-catenin signaling pathway [23–25]. Conversely, Sclerostin plays an antagonist role in bone formation along the sutures: Osteocytes near the bone fronts express Sclerostin, which binds to Wnt co-receptors Low-density lipoprotein receptor-related protein 5 and 6 (Lrp5 and Lrp6), preventing Wnt binding to them and thus antagonizing Wnt/β-catenin signaling in osteoblasts [26–28,49]. In this way, sites of high Wnt concentration at the sutures will be the ones where bone formation takes place. We assume that mesenchymal cells differentiation into osteoblasts will start once Wnt reaches a given threshold value. We model the concentration of Wnt and Sclerostin using a system of reaction diffusion equations that develops spatial patterns, which are stable in time and unstable in space, as follows (a prototype equation given in [35,50]):

$$\frac{\partial S_W}{\partial t} = C_K(\alpha_3 - \nu S_W + \gamma_1 S_W^2 S_R) + D_W \nabla^2 S_W \quad \text{(1-12a)}$$

$$\frac{\partial S_R}{\partial t} = C_K(\alpha_4 - \gamma_1 S_W^2 S_R) + D_R \nabla^2 S_R \quad \text{(1-12b)}$$

where C_K is the concentration of osteocytes near the bone fronts of each suture expressing Wnt and Sclerostin and S_W and S_R represent the concentration of Wnt and Sclerostin, respectively. The terms α_3 and α_4 quantify the production of Wnt and Sclerostin; ν is a constant that quantifies the inhibition in the production of S_W by its excess; γ_1 regulates the nonlinear interaction between the concentration of S_W - S_R and quantifies the activation or inhibition of each molecular factor and D_W and D_R are the diffusion coefficients of S_W and S_R, respectively.

The processes of bone formation at the sutures are dependent on the number of active osteoblasts synthetizing osteoid on the bone fronts. Since Wnt regulates mesenchymal cells differentiation into osteoblasts at these sites, we assume that osteoblasts concentration is dependent on Wnt, as follows:

$$C_{OS}(\bar{x}, t) = \epsilon(S_W) \quad \text{(1-13)}$$

where $C_{OS}(\bar{x}, t)$ is the concentration of osteoblasts at the sutures, ϵ is a constant that quantifies mesenchymal cells differentiation into osteoblasts through the action of Wnt and S_W is the concentration of Wnt. We assume that bone formation processes at the suture sites will start once osteoblasts concentration reaches a threshold concentration. The function $B_S(\bar{x})$ is an activation function that signals tissue differentiation at the sutures, and is given by:

$$B_S(\bar{x}) = \begin{cases} 1 \; if \; C_{OS}(\bar{x}, t) < C_{OST} \\ 0 \; other \; caso \end{cases} \quad \text{(1-14)}$$

where C_{OST} is the threshold concentration of osteoblasts where ossification has been achieved. Thus, the function $B_S(\bar{x})$ will be equal to 0 in locations where the suture has completely ossified and 1 in sites where the tissue remains membranous.

The processes of bone resorption are regulated by osteoclasts activity in flat bone fronts. As explained by Wada et al. [51], binding of RANKL to its receptor RANK is crucial for osteoclastogenesis and activation of mature osteoclasts. Since Osteoprotegerin (OPG) is an extracellular matrix protein that negatively regulates RANKL binding to RANK, osteoclasts activity diminishes with higher OPG concentrations. Thus, osteoclasts differentiation from hematopoietic stem cells is regulated by both RANKL and OPG spatial distributions. According to [23,31], the Wnt/β-catenin signaling pathway not only plays a major role in the differentiation of mesenchymal cells into osteoblasts. In addition to this, this pathway induces OPG expression by osteoblasts in a proportional manner, promoting the ability of these cells to inhibit osteoclast differentiation by releasing higher amounts of OPG as a result of higher Wnt expression signaling osteoblasts differentiation. Therefore, we assume that sites of bone resorption will be those with low Wnt concentration (high Sclerostin concentration), since low OPG concentrations will be present and higher amounts of RANKL will bind to RANK. We model the processes of bone resorption on one bone front as the reflection of the bone formation patterns obtained in the opposing bone front (see **Fig. 1-5a** and **1-5b**). These processes of bone formation and resorption, together with the continuous narrowing of the suture through bone formation processes regulated by TGF-β2 and TGF-β3 concentrations (see Eqs. (1-1) – (1-11)), generate an interdigitated suture (see **Fig. 1-5c** and **1-5d**).

Figure 1-5: Schematic showing the process of suture interdigitation in a bi-dimensional segment of a bone-suture-bone interface. (a) Assumed initial pattern of bone formation driven by locations of high Wnt concentration (bone in light yellow, suture in light pink). (b) Resulting pattern of bone resorption. We can see how bone formation patterns on one bone front are reflected on the opposing front as resorption sites, as shown with blue arrows. New sites of suture growth are displayed in dark pink. (c) Suture pattern obtained from bone formation and resorption events. (d) Resulting pattern of suture interdigitation after

considering the reduction in suture width produced by bone formation events regulated by TGF-β2 and TGF-β3 concentrations. (Bone in light yellow, suture in light pink).

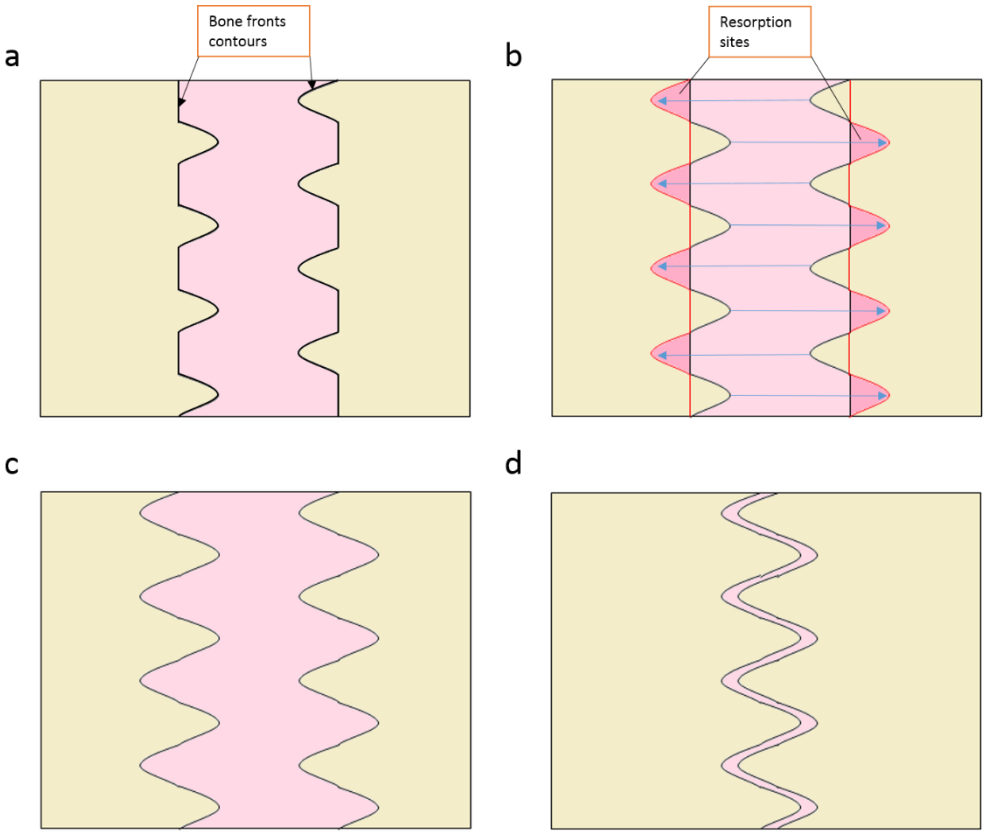

1.4 Numerical implementation

The set of equations (1.1)–(1-14) were implemented in a FORTRAN subroutine and numerically solved using the finite element method with a Newton–Raphson scheme. The proposed examples were solved in a Laptop of 8 GB and 2.0 GHz processor speed. The computer simulation was carried out in an incremental iterative scheme which allows solving, computationally, the evolution of the concentration of each molecular factor.

1.4.1 Implementation of the second developmental stage

We initially made the computational implementation of the second developmental stage: The growth of the flat bones and formation of sutures. For this we used a geometric approximation of the calvaria during prenatal development. **Fig. 1-6** show the finite

elements mesh employed to solve the problem and the geometric parameters defined in the simulation, which are based on the growth charts given by [52] for a fetus in the fourteenth week of gestation. We follow the results obtained by [35], where six ossification centers were generated through the spatio-temporal concentrations of BMP2 and Noggin. Equations (1-1)-(1-11) were numerically solved during a time lapse of 33 months: 9 months during prenatal development and 24 months corresponding to infancy. The mesenchymal tissue, where no ossification has been achieved yet, is assumed as a structural matrix with an initial concentration of mesenchymal cells equal to $4x10^6 \frac{cell}{ml}$ [53]. The flow conditions, for each molecular factor in the boundary (TGF-β2 and TGF-β3), are assumed null. This assumption is based on that, under the calvaria (in the condrocraneal region), endochondral ossification has already existed. Hence, permeability is decreased and a barrier between the condrocraneal and vicerocraneal regions and the membranous neurocranium is formed [54]. Similarly, we assumed a null initial concentration of TGF-β2 and TGF-β3 in the entire domain. Therefore, TGF-β2 production by osteoblasts will begin along the ossification fronts of each previously developed ossification center.

1.4.2 Implementation of the third developmental stage

For the events of suture interdigitation and fusion, we defined a bi-dimensional domain (two spatial dimensions) considering a segment of the bone-suture-bone interface of the sagittal suture from a newborn calvaria (see **Fig. 1-7**), with a suture width of 5 mm, as measured by Mitchell et al. [55] for newborns at zero months of age. This decision was made for simplification purposes on the computational implementation. The sagittal suture has been previously employed in various computational models of suture interdigitation [37,39]. Thus, it gives an ideal framework for results assessment. Moreover, this suture is shaped by the parietal bones, which have the same embryonic tissue origin (paraxial mesodermal-derived), and a symmetry in their biomechanical environment given by a less complex geometry as the one present in other sutures. We restrict the implementation to the outermost part of the sagittal suture and obtain the time evolution of both Wnt and Sclerostin concentrations on the bi-dimensional domain, which determine the sites of bone formation along the suture. The initial concentration of Wnt and Sclerostin are randomly distributed on the suture tissue, with a 10% disturbance over the steady-state concentration, given by $(S_W^*, S_R^*) = (1.0,0.9)\left[\frac{ng}{ml}\right]$ (see Appendix A). Equations (1-12)-(1-14) were numerically solved

during a time lapse of 24 months corresponding to infancy. The flux of each molecule across the boundary is assumed null, following the reasons previously explained [54].

The sites of bone resorption are achieved by performing a natural cubic spline interpolation of the bone fronts ossification patterns obtained from Wnt and Sclerostin concentrations in the bi-dimensional domain. These ossification patterns are given by the shape of the contours separating ossified and membranous tissue on each side of the suture (see **Fig. 1-5a**), and can be seen as mathematical functions representing the shape of each bone front after Wnt driven ossification. The spline interpolation gives a set of polynomials which allow the reconstruction of each bone front contour, where resorption sites result from plotting the contour function of one bone front on the opposing one (see **Fig. 1-5b**).

1.4.3 Suture interdigitation in the 3d model

The ossification patterns obtained from the time evolution of Wnt and Sclerostin concentrations in the bi-dimensional domain used for the sagittal suture during infancy (24 months) are mapped to the entire calvaria (3d domain used in the second developmental stage). This mapping ensures that bone formation and resorption processes along the ossification fronts of each flat bone are regulated by both TGF-β2-TGF-β3 and Wnt-Sclerostin reaction diffusion systems. This procedure is made considering that flat bones can be modelled as thin-walled shells, where thickness is negligible in comparison to the other two dimensions. Therefore, we can assume that the entire calvaria can be represented as bi-dimensional domains for each bone-suture-bone interface representing each of the sutures.

Figure 1-6: (a) Prenatal Skull, (b) Simplified geometry with 8353 nodes and 16549 triangular elements. (c) and (d). Geometric relationships used in the computational model. a = 32 mm, b = 48 mm (b/a = 1.5), c = 16 mm, d = 9.6 mm and r = 8 mm.

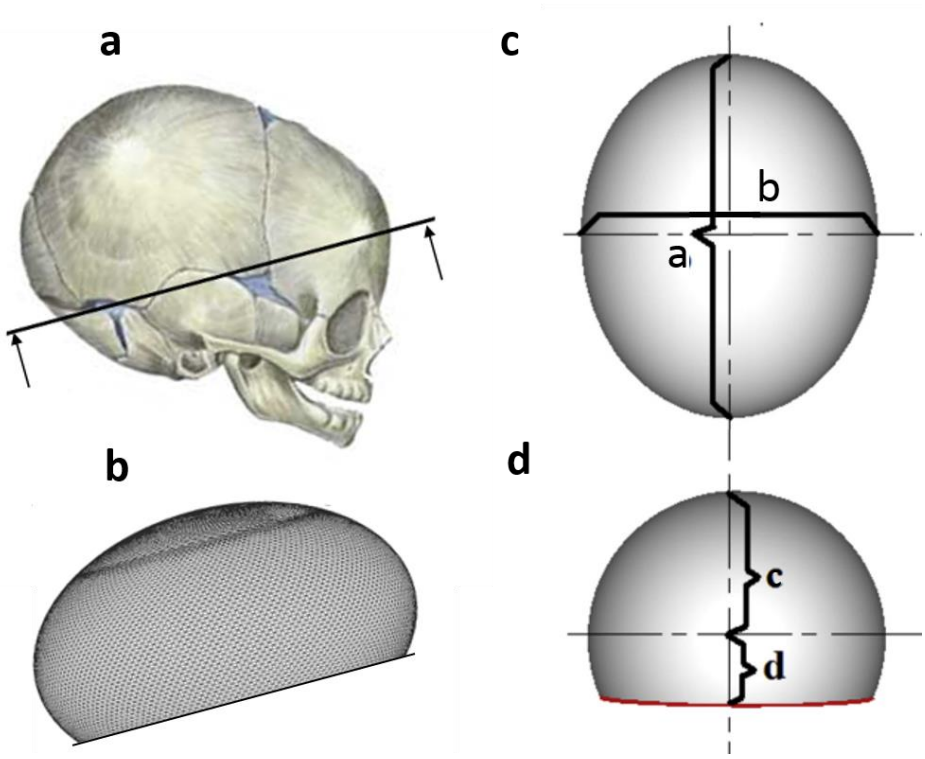
a
b
c
d
b
a
c
d

Figure 1-7: (a) Coronal view of the neonatal calvaria. Adapted from [56]. (b) Segment of the sagittal suture considered. (c) Bi-dimensional mesh with 15140 nodes and 29822 triangular elements.

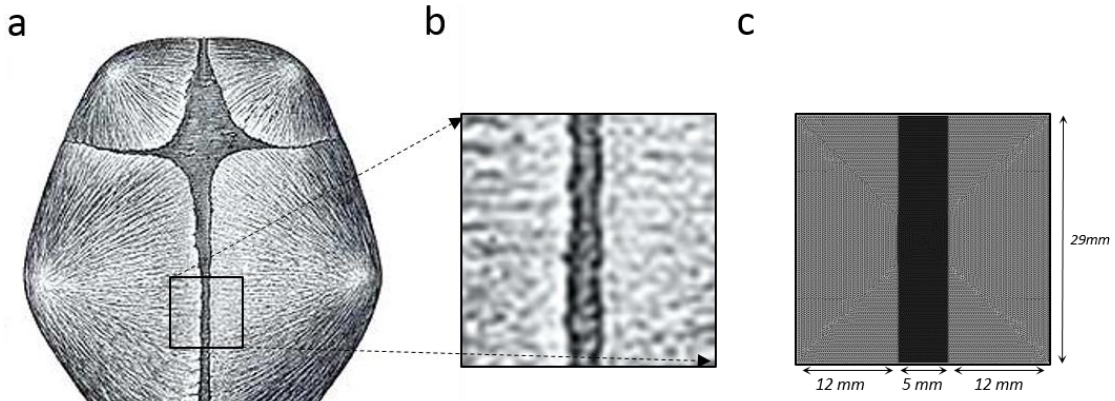

1.4.4 Parameters

Table 1-1 summarizes the parameters used in the mathematical model. Most of the parameters were found by trial and error numerical experimentation, since no previous reports have been made for them in the literature. Furthermore, a sensitivity analysis was carried out to assess parameter robustness for different initial conditions. Hence, the parameter values used correspond to the ones needed for accurately simulating the considered biological events.

Table 1-1: Parameters used in the model.

Parameters	Value	Units	Reference
α	$1.7(x10^{-15})$	$\frac{ng}{cell.s}$	[34]
S_{TD-i}	1.5	$\frac{ng}{ml}$	[34]
n	10	Dimensionless	[34]
β	0	Dimensionless	[34]
t_D	3600	s	[34]
D_{D-i}	$8.66(x10^{-5})$	$\frac{mm^2}{s}$	[34]

γ_i	$2.5 - 10(x10^{-8})$	$\frac{ml^2}{cell.s.ng}$	Numerical experimentation
C_m	$4(x10^6)$	$\frac{cell}{ml}$	[53]
S_{TG}	1.2	$\frac{ng}{ml}$	[57]
k	0.5	Dimensionless	Numerical experimentation
t_G	3600	s	Numerical experimentation
D_G	$3.46(x10^{-6})$	$\frac{mm^2}{s}$	Numerical experimentation
m	10	Dimensionless	Numerical experimentation
C_{OT}	100	$\frac{cell}{ml}$	Numerical experimentation
ξ	0.15	$\frac{ng}{ml}$	Numerical experimentation
λ	500	$\frac{cell}{ng}$	Numerical experimentation
C_K	$10.5(x10^6)$	$\frac{cell}{ml}$	[58]
ν	$6.92(x10^{-13})$	$\frac{ml}{cell.s}$	Numerical experimentation
γ_1	$6.92(x10^{-13})$	$\frac{ml^3}{s.cell.ng^2}$	Numerical experimentation
α_3	$6.92(x10^{-14})$	$\frac{ng}{cell.s}$	Numerical experimentation
α_4	$6.23(x10^{-13})$	$\frac{ng}{cell.s}$	Numerical experimentation
D_W	$3.70(x10^{-6})$	$\frac{mm^2}{s}$	[59]
D_R	$4.30(x10^{-7})$	$\frac{mm^2}{s}$	[59]
ϵ	97.56	$\frac{cell}{ng}$	Numerical experimentation
C_{OST}	100	$\frac{cell}{ml}$	Numerical experimentation

Based on the performed sensitivity analysis, the following parameters were found to be most critical to the model predictions. A biological interpretation of them is given below:

- α quantifies TGF-β2 production by osteoblasts. It indicates how much TGF-β2 mass is produced by each cell per second. Increasing this value led to higher TGF-β2 concentrations and higher ossification rates along the flat bone ossification fronts.

- S_{TD-i} and S_{TG} correspond to TGF-β2 and TGF-β3 saturation concentrations. Thus, the production of these factors from osteoblast and mesenchymal cells at a domain point of analysis is limited if TGF-β2 and TGF-β3 concentrations are near the defined saturation values. Increasing this factors induces higher TGF-β2 and TGF-β3 concentrations.
- D_{D-i} and D_G correspond to TGF-β2 and TGF-β3 diffusion coefficients. Increasing these values generated instabilities in the response, while lower values reduce ossification velocities along the bone fronts.
- γ_i quantifies the production of TGF-β3 by mesenchymal cells located at the sutures. Increasing this parameter's value induced higher TGF-β3 production, which inhibited mesenchymal cells differentiation at the flat bone osteogenic fronts. Consequently, less bone was formed at the sutures and bigger regions of the calvaria remained unossified.
- C_{OT} refers to the minimum osteoblast concentration from which it is assumed a domain point has ossified. Increasing its value led to lower ossification rates along the bone fronts, while its decrease led to higher bone formation rates.
- ξ refers to the minimum TGF-β2 concentration detected by mesenchymal cells en a domain point which triggers TGF-β3 production. By decreasing this value, TGF-β3 was produce earlier in time in response to lower TGF-β2 concentrations at the sutures. Hence, bone formation was greatly inhibited and bigger regions remained unossified at the end of prenatal development. Increasing this value led to a delayed production of TGF-β3, thus causing a greater narrowing of the sutures and in some cases the complete obliteration of them before the end of prenatal development.
- λ quantifies mesenchymal cells differentiation following the difference between TGF-β2 and TGF-β3 concentration at a domain point of analysis. Increasing this value led to higher ossification rates at the osteogenic fronts of each flat bone.
- The constants ν, γ_1, α_3 and α_4 were found using the values of the parameters β, e, c and d from the non-dimensional model (see equations (A3a) and (A3b) in Appendix A). α_3 and α_4 indicate the amount of Wnt and Sclerostin mass produced by each osteocyte per second. ν indicates the volume of Wnt consumed by each mesenchymal cell per second and γ_1 refers to the nonlinear interaction between Wnt and Sclerostin. These parameter values determined the shape of the

concentration patterns of Wnt and Sclerostin which generated bone formation and resorption regions along the sutures.

- The constant ϵ quantifies mesenchymal cells differentiation into osteoblast through the action of Wnt. Increasing these value induced a higher rate of differentiation and thus, higher ossification speed along the sutures.
- C_{OST} refers to the minimum osteoblast concentration in the sutures from which it is assumed a domain point has ossified. Increasing its value led to lower ossification rates along the bone fronts, while its decrease led to higher bone formation rates.

1.5 Results

1.5.1 Second event: Bone growth and suture formation

Following the formation of the primary ossification centers, osteoblasts at the bones margins of each flat bone release the protein TGF-β2. **Fig. 1-8** shows the time evolution of TGF-β2 in frontal bones (TGF-β2-3 and TGF-β2-4). The concentration of TGF-β2 increases up to a value of $1.4\,\frac{ng}{ml}$.

Figure 1-8: Time evolution of the TGF-β2 concentration for the frontal bones during prenatal development. The areas of initial release of TGF-β2 correspond to the primary ossification centers. (a) Right frontal bone. (b) Left frontal bone. Time (t) is expressed in months (m).

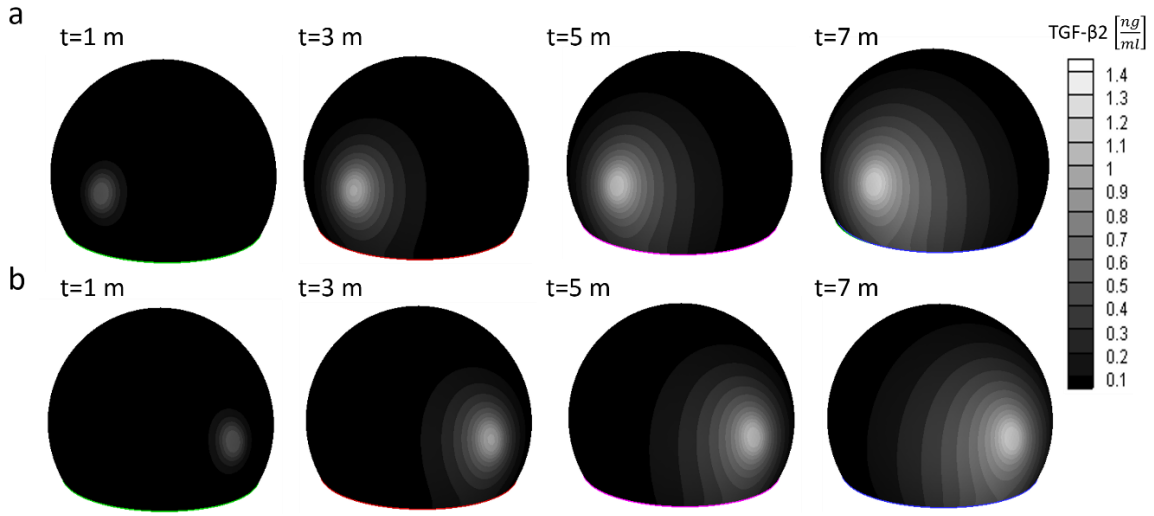

Once TGF-β2 concentration surpasses a threshold value at the sutures, mesenchymal cells located there start releasing TGF-β3 [17], inhibiting the differentiation of mesenchymal cells into osteoblasts at the bone fronts of each suture [21,22]. Thus, flat bone growth is dependent of both TGF-β2 and TGF-β3 concentrations (see **Fig. 1-9**).

Figure 1-9: TGF-β3 concentration and bone formation during normal prenatal development. (a) Time evolution of TGF-β3. Areas of high TGF-β3 concentration defined the sites of suture formation. (b) Time evolution of bone formation of the flat bones during prenatal development. Flat bones grow radially following the diffusion of the molecule TGF-β2 and their growth diminishes due to the expression of TGF-β3 by the mesenchymal cells at the sutures sites. The bones leave wide spaces between them, called fontanels and sutures, which coincide with areas with TGFβ-3 concentrations higher than 0.6 ng/ml. Therefore, premature suture ossification is inhibit. Time (t) is expressed in months (m).

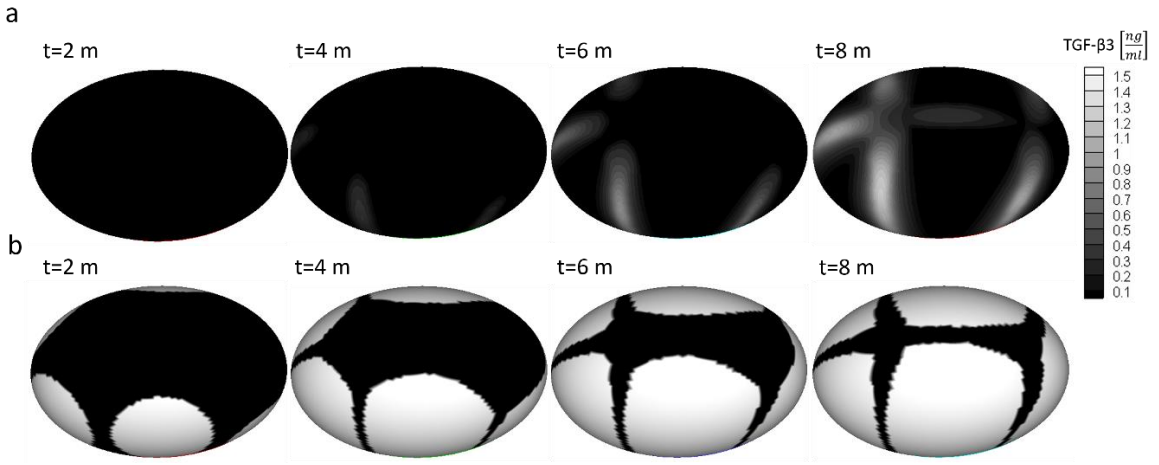

Fig. 1-10 shows the influence of different values of γ_4(Constant that quantifies emission of TGF-β3 by mesenchymal cells at the metopic suture) on the ossification process taking place at the metopic suture. Note that values of γ_4 lower than $7.5\,x10^{-8}\frac{ml^2}{cel.s.ng}$ induce premature fusion of this suture. Hence, this value of γ_4 is the threshold between a prematurely fused and a patent cranial suture in the performed simulation, meaning that

concentrations higher than this will inhibit premature suture fusion. Similarly, concentrations of TGF-β3 higher than $0.04\frac{ng}{ml}$ inhibit premature fusion of the metopic suture.

Figure 1-10: Results of TGF-β3 concentration and bone formation at the metopic suture for different values of the constant $\boldsymbol{\gamma_4}$ in equation (1-2) for time t=3.5 months prenatal. (a) TGF-β3 concentration in the metopic suture. (b) Bone formation in the metopic suture. Note how the increment of $\boldsymbol{\gamma_4}$ regulates bone formation at the site of the metopic suture, going from premature fusion to patency. Units of $\boldsymbol{\gamma_4}$ are in $\left[\mathbf{10^{-8}}\frac{\boldsymbol{ml^2}}{\boldsymbol{cel.s.ng}}\right]$.

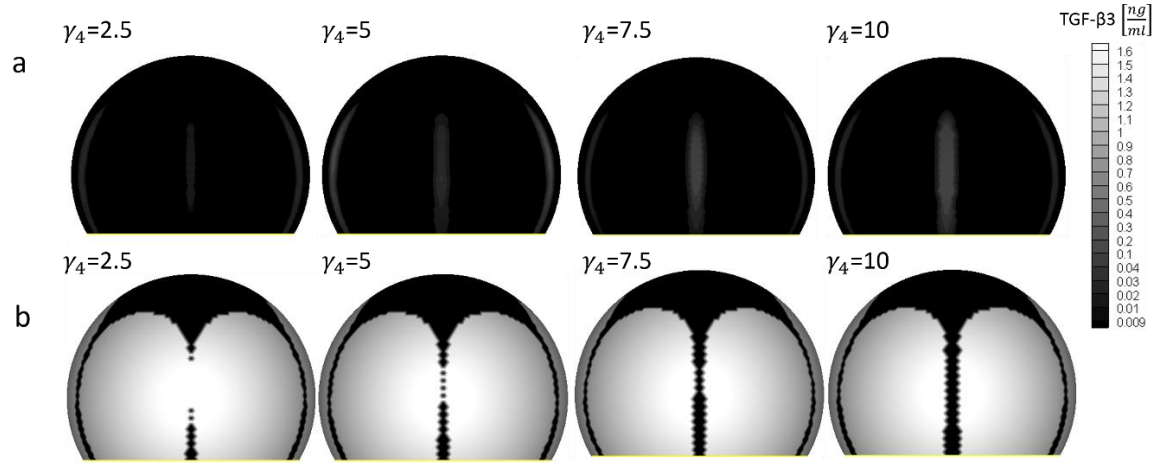

1.5.2 Third event: Suture interdigitation and fusion

Fig. 1-11 shows the steady state response of the concentrations of Wnt and Sclerostin in the bi-dimensional domain defined for the sagittal suture. The areas of high Wnt concentration correspond to the ones with low Sclerostin concentration. Bone formation is dependent on the concentration of osteoblasts at the suture borders, which is controlled by Wnt. Once Wnt reaches a threshold value, mesenchymal cells differentiation into osteoblasts starts. Note that areas of high Wnt concentration will be the ones where mesenchymal differentiation takes place, and therefore where bone formation will begin. **Fig. 1-12** shows the time evolution of the process of interdigitation regulated by bone formation and resorption events during infancy. Note the correspondence between areas of high Wnt concentration and bone formation events and areas of high Sclerostin concentration (low Wnt) with bone resorption events.

Figure 1-11: Steady state response of the concentration of Wnt and Sclerostin for a bi-dimensional segment of the sagittal suture.

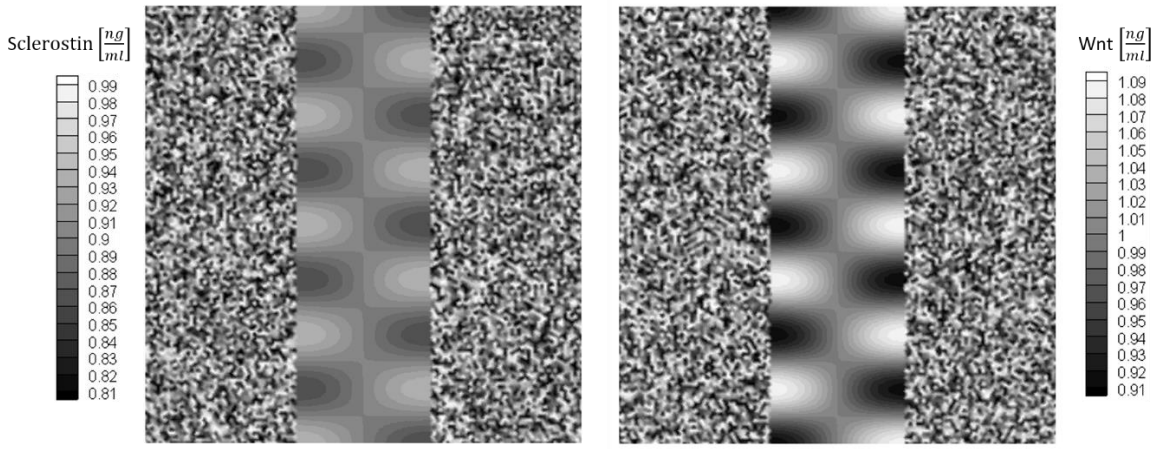

Figure 1-12: Results of process of suture interdigitation during infancy for a bi-dimensional segment of the sagittal suture. Note the beginning of interdigitation at 12 months of age and the continuous narrowing of the suture throughout infancy. Suture is depicted in black, bone in white. Time (t) is expressed in months (m).

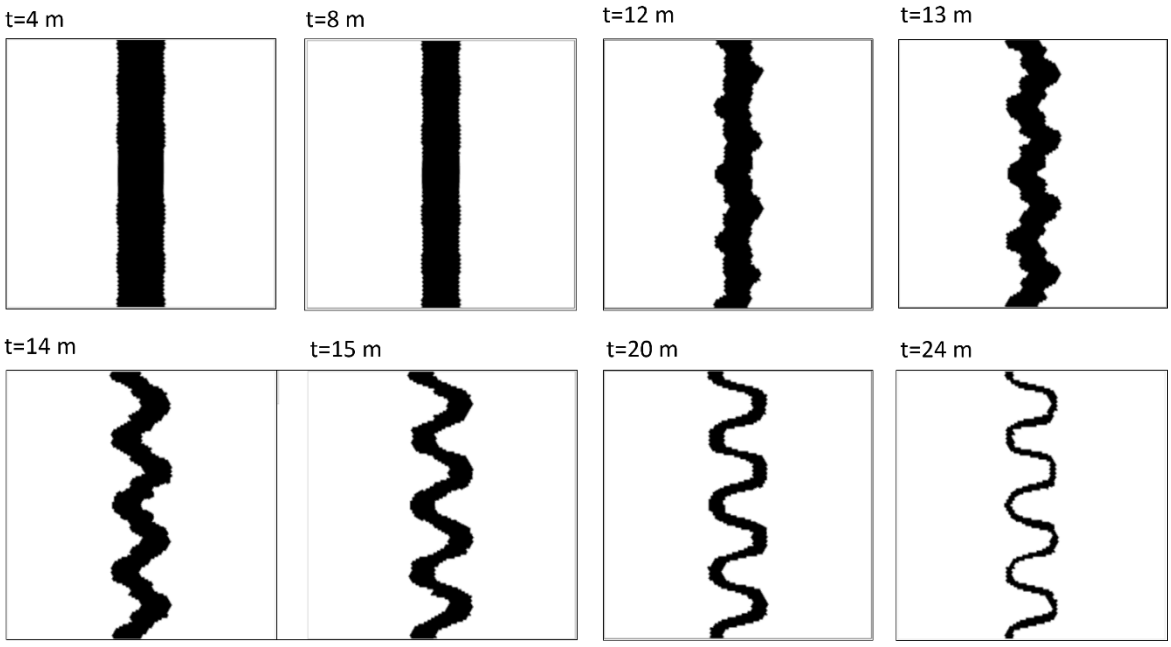

The results from the bi-dimensional model are then mapped into the geometry of the entire calvaria. **Fig. 1-13** and **Fig. 1-14** show the results from the simulation of suture interdigitation and fusion in the calvaria during the first two years of postnatal development through the combined action of TGF-β2 and TGF-β3 concentrations and the mapped ossification patterns obtained from Wnt and Sclerostin concentrations in the bi-dimensional domain of the sagittal suture. Note the closure of the anterior and posterior fontanels and the fusion of the metopic suture at different developmental ages, as well as the onset of interdigitation along remaining sutures. **Fig. 1-15** shows a morphological comparison between flat bones and sutures obtained in the simulations and an adult calvaria.

Figure 1-13: Time evolution of the process of suture interdigitation and fusion during postnatal development for the coronal and sagittal sutures. Time (t) is expressed in months (m).

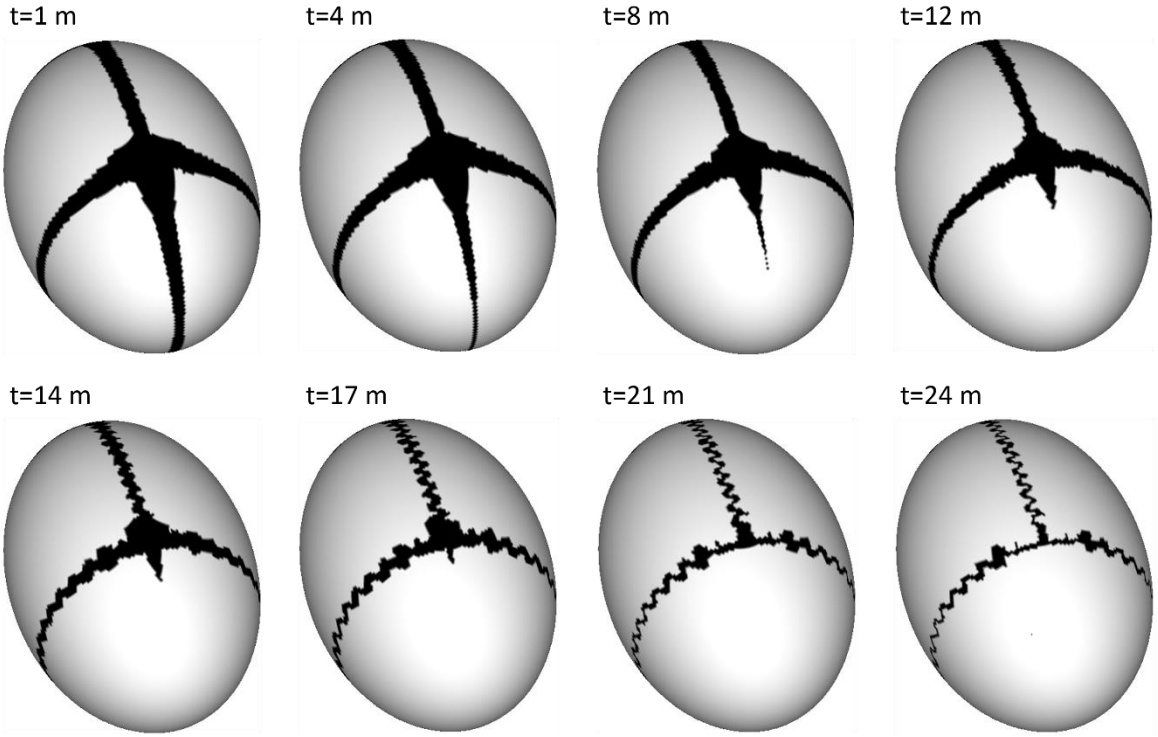

Figure 1-14: Time evolution of the process of suture interdigitation and fusion during postnatal development for the lambdoid and sagittal sutures. Time (t) is expressed in months (m).

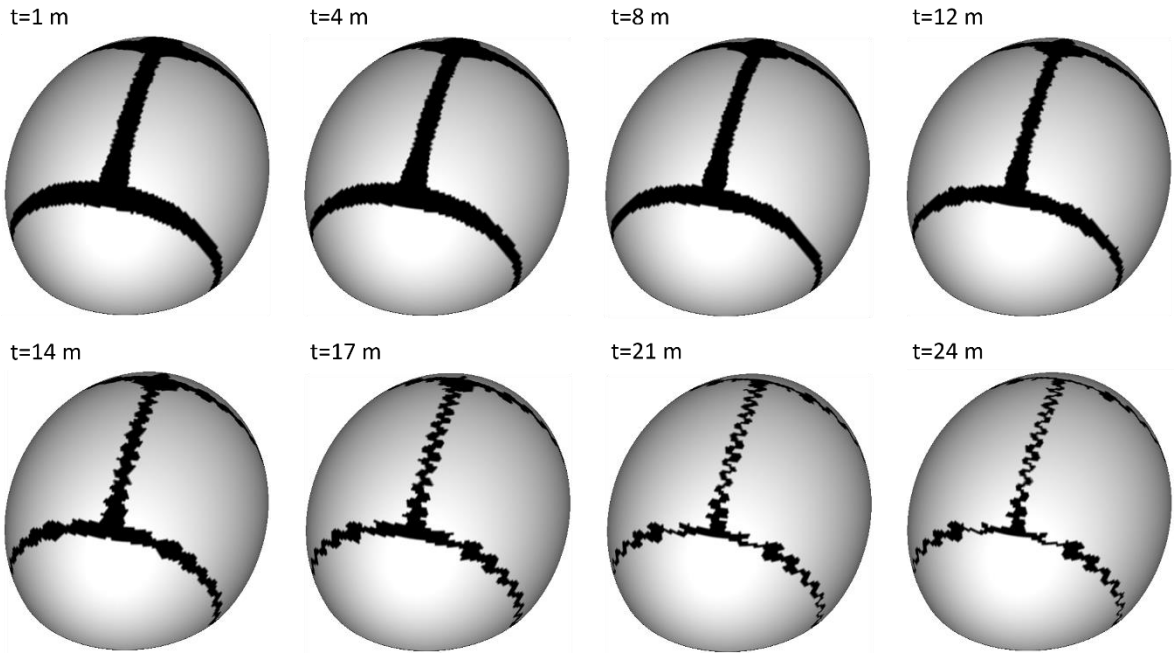

Figure 1-15: Morphological comparison between simulation results and adult calvaria. (a) Simulation results for suture interdigitation and fusion during infancy. (b) Adult calvaria.

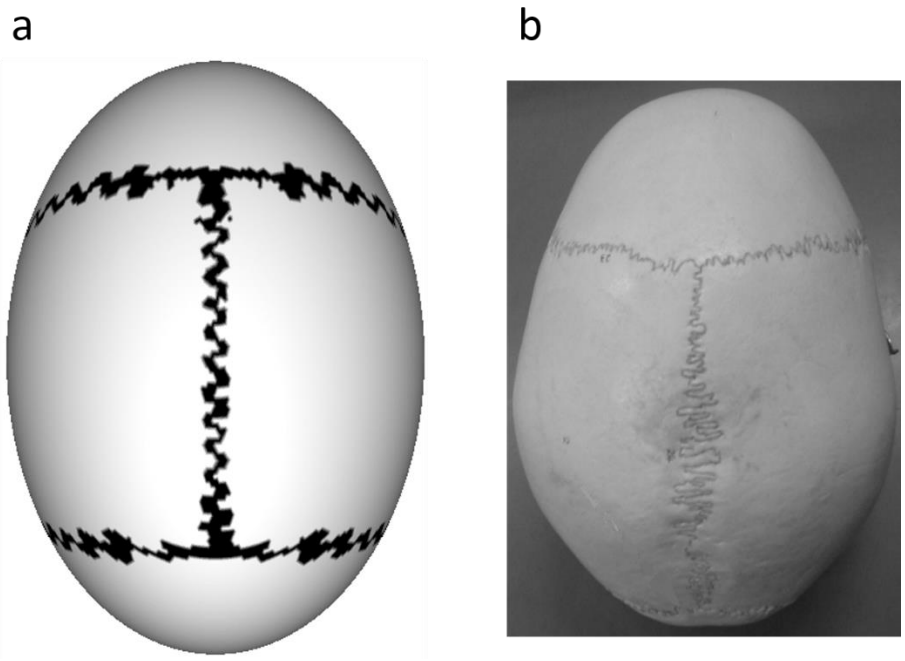

1.6 Discussion

This article has developed a mathematical model of the formation of the flat bones and sutures of the calvaria using a biochemical approximation that regulates bone formation and resorption processes throughout prenatal development and infancy. To do this, we have assumed three consecutive events. The first one takes into account the formation of the primary ossification centers driven by the concentrations of BMP2 and Noggin, an event previously simulated in_[35]. The second event implies that bone growth and suture formation are controlled by TGF-β2 and TGF-β3. The third event considers the processes of suture interdigitation and fusion, which are given by a complex regulation between bone formation and resorption processes in the calvarial sutures. We assume that osteocytes located near the bone fronts of each suture express Wnt and Sclerostin, where high Wnt concentrations promote bone formation by inducing mesenchymal cells differentiation into osteoblasts and low Wnt concentrations triggers bone resorption by promoting osteoclastogenesis at opposing bone front sites where no Wnt driven ossification took

place. In this way, the resulting patterns of bone formation and resorption, together with the effects of TGF-β2 TGF-β3, generate interdigitated sutures.

The second stage of the process takes into account the proteins TGF-β2 and TGF-β3. The model is able to simulate how the diffusion of these molecules (see **Fig. 1-8** and **1-9a**) regulate bone formation at the bone fronts and the subsequent formation of suture and fontanels (see **Fig. 1-9b**). It is noteworthy to mention that adjacent mesenchymal cells differentiation is not only regulated by TGF-β2, since other molecules such as the FGFs, Msx2 and GPC have been demonstrated to impact bone formation processes [48,60–62]. Nonetheless, the hypothesis employed in this article regarding radial growth of the flat bones has a good correlation with flat bone morphogenesis [48].

The processes of suture formation and patency have been the subject of a vast amount of research. Premature fusion of the cranial sutures has been achieved in both *in vivo* and *in vitro* studies. Not only alterations in the biochemical expression of molecules such as TGFs and FGFs have been made [5,17,18,60,62], but also mechanical factors such as compressive stresses [63] have been employed and shown to have an effect on cranial suture fate. This gives the idea that suture formation is defined by a complex interaction between genetic, biochemical and environmental factors. The most prevalent hypothesis so far states that sutural fate (fusion versus patency) is predominantly regulated by the dura mater directly underlying a given cranial suture [14]. Regional dura mater releases both osteogenic inhibitors and promoters to the suture complex such as FGFs, FGFRs, TGFs and bone-associated extracellular matrix molecules, which are involved in suture fusion and patency [17]. This hypothesis was corroborated by Greenwald et al. [14], who demonstrated that osteogenic cytokines and bone-associated molecules expression are potently up-regulated in the dura mater associated with the rat posterior frontal suture (programmed to fuse), while they are down-regulated on the sagittal suture (remains patent). These results indicate that the dura mater underlying the rat sagittal suture became imprinted with a signal preventing osteogenic processes on the suture. This biochemical signal is inherent to the regional dura mater, as it has been shown by *in vitro* and *in vivo* studies, where underlying dura of normally unfused sutures maintained patency when implanted below sutures physiologically destined to fuse [64–66]. The results from our simulations agree with these hypotheses by showing how regional alterations in TGF-β3

expression determine the fate of each of the sutures in the calvaria. Concentrations of TGF-β3 lower than $0.04\frac{ng}{ml}$ induce premature fusion of the sutures, where, initially, a single point shows obliteration and continues its propagation along the suture line, just like it has been experimentally demonstrated [67] (see **Fig. 1-10**). Additionally, these results agree with experimental evidence regarding suture maintenance and premature fusion [14], suggesting a complex regulatory mechanism between osteoinductive and osteoinhibitory signals coming from the regional dura mater and acting on each of the cranial sutures. Our hypothesis proposes that this mechanism relies on the ability of mesenchymal cells to react to the increasing concentration of TGF-β2, coming from opposing bone fronts at each suture location, by expressing TGF-β3. Therefore, premature fusion of the sutures during prenatal development might be caused by alterations in transduction processes on these cells, interfering with their ability to express TGF-β3. This could explain the premature fusion of sutures seen in pathologies like Non-syndromic Craniosynostosis, where no single genetic mutation has been found that causes the condition [40]. Thus, our model gives an alternate explanation to this biological process, which should be validated through future experimental studies. However, the above assumption doesn't account for suture fusion after birth. The time of fusion is variable among different sutures, e.g., the metopic suture normally closes before nine months of age [10], while the remaining sutures have been found open even after thirty years of age [11]. Hence, we propose that the metopic suture might have a down-regulation of TGF-β3 expression, or perhaps a decrease sensory ability of incoming gradients from TGF-β2 expressed at the bone fronts of the left and frontal bones. Thus, after sutures have been formed (by the end of prenatal development), TGF-β3 expression must be down-regulated on the metopic suture for fusion to occur in infancy, while its expression at the other sutures remains the same. Considering this hypothesis, we down-regulated TGF-β3 expression on the metopic suture and simulated its ossification, which begins at approximately seven months of age and is completed at 12 months of age (see **Fig. 1-13**).

Previous computational models related to the suture formation [34,36] suggest the existence of an unique morphogen for each growing flat bone, which inhibits the growth of adjacent bones at the suture locations. Even though this hypothesis was computationally simulated, it did not take into account the presence of osteoinhibitory signals (like TGF-β3) able to stop the bone formation in the suture regions [17,19–22,68]. Additionally, the results

obtained in the model developed in this work show a bone and suture morphology closer to reality than the ones obtained in previous models (see **Fig. 1-16**). Considering both osteoinductive and osteoinhibitory biochemical signals in this work, helps to better match the actual processes of bone formation in the cranial vault. These processes depend on the spatio-temporal variation of biochemical signals, which alters the proliferation, differentiation and apoptosis levels of osteogenic cells.

Figure 1-16: Results comparison between different computational studies. a) Results for bone formation in the cranial vault in the mouse [36]. We can see the formation of each flat bone as well as the formation of fontanels. b) Bone formation in the human cranial vault of our previous computational study [34], which considers bone growth mediated by transcription factor DLX5. c) Results of bone and suture formation in this work. d) Pictorial view of the real human cranial vault after birth. Note the morphological similarities between the results from this work and the real calvaria in terms of flat bones and sutures location and morphology.

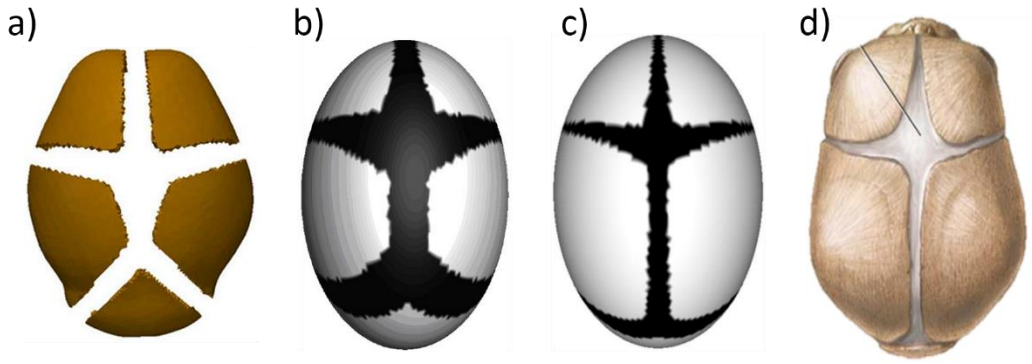

Our hypothesis proposes that the initial stages of suture interdigitation in infancy are achieved through two uncoupled processes: Suture width reduction by the overall radial bone growth controlled by TGF-β3 and TGF-β2 concentrations, and a local interaction between bone formation and resorption processes taking place at opposing bone fronts through the action of Wnt and Sclerostin concentrations patterns along the sutures. The results obtained in the interdigitation process described in this article show a strict regulation between bone formation and resorption events at the sutures. Our hypothesis proposes that these processes aren't independent, but rely on the same molecular

pathway: The Wnt/β-catenin signaling pathway [23,31]. Hence, interdigitation is dependent on Wnt and Sclerostin concentrations along the sutures, where high Wnt concentrations (low Sclerostin) induce bone formation and low Wnt concentrations (High Sclerostin) promote bone resorption. Interestingly, the system of reaction diffusion equations employed in this stage produces concentration patterns of Wnt distributed in such a way, that sites of high Wnt concentration on one bone front are confronted by low Wnt concentrations on the opposing bone front (see **Fig. 1-11**). Additionally, bone fronts on each suture will experience intercalated areas of high and low Wnt concentrations along the suture line. These conditions generate intercalated bone formation and resorption events at the suture borders, where sites of bone formation on one front have a resorption cavity in the opposing bone front. Consequently, no obliteration points will arise along the suture, as seen in normal adult sutures (see **Fig. 1-15b**). We propose that these patterns of bone formation and resorption might be controlled by osteoblasts on the bone front where bone formation takes place. Hence, not only do osteoblasts synthetize osteoid on one bone front, but also induce osteoclastogenesis on the opposing front, which, as previously stated, will have a low OPG concentration caused by high Sclerostin concentration. Thus, Osteoblasts expression of RANKL on the bone forming front will bind in a higher manner to RANK receptors located on the opposing bone fronts, promoting a higher degree of osteoclastogenesis. Therefore, a greater number of active osteoclasts will produce a resorption cavity on these sites, and the suture will be able to maintain its patency. In addition, suture narrowing is dependent on bone formation processes driven by TGF-β2 and TGF-β3 concentrations, which account for a gradual decrease in suture width, from 5 mm to less than 1 mm, as seen in **Fig. 1-12**. These findings suggest that *in vivo* suture interdigitation is dependent on several molecular pathways regulating bone formation and resorption events along the sutures. We suggest that the locally defined concentration patterns of TGF-β2, TGF-β3, Wnt and Sclerostin obtained in this paper might be similar to the ones present on human calvarial sutures. This is of course our proposed explanation to the processes generating suture interdigitation, considering that no alternative explanation currently exist about what causes it.

Previous experimental studies have proven that Wnt and Sclerostin perform opposite roles in bone homeostasis by promoting bone formation and resorption events, respectively [23–29]. These effects have been elucidated in different types of bones in both humans and

animal models. However, no single study has specifically conduct research on the effects of these molecules on cranial development and suture interdigitation. Hence, even though their action might be critical for the activation of osteoblasts and osteoclasts at the sutures, further experimental work should be focused on revealing the spatio-temporal variations of the concentrations of these biochemical factors at the sutures and their effects on bone formation and resorption events in the calvaria.

The molecules considered in this work for modeling flat bone growth and suture formation and interdigitation have been chosen based on previous experimental evidence accounting for their role on bone formation and resorption events in the calvaria. These molecules are growth factors present in the extracellular domain which have specific receptors accounting for specific signaling pathways. Thus, it seems that they play a fundamental role on bone and suture morphogenesis. Therefore, we believed that the chosen molecules are prototype molecules which act in a similar way to what might be occurring during the biological processes considered. Nevertheless, since the actual mechanisms underlying the modelled processes must be heterogeneous in nature and other molecules could be equally or more important in these biological events, this model is a simplification of reality. For this reason it should be listed, as in any other mathematical model, its drawbacks and limitations.

The first limitation refers to cell motion in the calvaria. We have assumed that mesenchymal cells migration is low since they are immersed in the extracellular matrix. Hence, our hypothesis considers that mesenchymal cells differentiate to osteoblasts without a large movement from their initial position.

The second limitation takes into account the number of stages in the formation of bones and sutures of the skull. Here we have assumed three stages, involving six biochemical signals: Noggin, BMP2, in the first stage; TGF-β2 and TGF-β3 in the second; Wnt and Sclerostin in the third. It is important to recognize that these molecular factors are not the only ones acting in these processes. Others factors such as BMPs, TGF-βs, FGFs, FGFRs, WIF1, RUNX2, DLX5 and MSX2 have also been implicated in calvarial morphogenesis [17,61,69–71].

The third limitation refers to the type of boundary conditions and the initial conditions. We have chosen null flow in the domain of study. This is based on that, prior to the formation of the primary ossification centers, the skull is made up by the membranous neurocranium (cranial vault) and the cartilaginous neurocranium (skull base). When formation of the primary ossification centers begins, the cartilaginous neurocranium already has two weeks of ossification [54]. Therefore, the boundary between these two regions will have, on one hand, mesenchymal cells from the cranial vault, and on the other, osteoblasts that have already started to form the bones of the face and skull base. Thus, the flow of molecular factors from and toward the cranial vault may be negligible, since the diffusion coefficient of the ossified side is lower. Likewise, since initial conditions are unknown, we have chosen null initial conditions for TGF-β2 and TGF-β3. Other limitation is the geometry used. The defined geometry for the tridimensional domain is a simplification of the graphs presented by Sadler for a fetus in the fourteenth week of gestation [54].

Another limitation was the exclusion of the effects of brain growth and masticatory function in the mathematical model. Since the spatio-temporal patterns produced by the system of reaction diffusion equations between BMP2 and Noggin are highly dependent on domain geometry, the rapid expansion of the brain [3] during prenatal development can alter the exact location of the centers of ossification. Additionally, it has been shown that presence or absence of brain growth changes suture positioning, bone density and collagen fiber orientation [15]. Hence, one possible impact of brain growth on bone formation at the sutures is the one described by Ogle et al. [5], who showed that mechanical forces coming from brain growth are sensed as quasi-static strains at the dura mater sites. Similarly, suture morphological complexity have been linked with stress and strain distributions present throughout the skull. Experimental studies have shown how the beginning of the masticatory function changes the mechanical environment in each of the sutures, mainly by generating cyclical compression and tensional load regimes, where the existence of compressive loads is associated to the onset of interdigitations [72–75]. Likewise, *in vivo* studies of pig sutures suggest that interdigitation complexity is linked to the presence of compressive strains oriented perpendicular to the suture line, while tensional strains usually produce butt ended sutures [75]. Given this, the biochemical hypotheses of suture formation and interdigitation described in this article should be complemented with a mechanobiological analysis of stress and strain that considers the effects of both quasi-

static strains and cyclic tensile and compressive loads (coming from brain growth and masticatory function) on bone formation and resorption processes. In this manner, a more complex pattern of ossification along the sutures might be produced, as the one displayed in **Fig. 1-15b**, where sutures exhibit variable amplitude, fractality and positioning throughout the calvaria.

The last limitation refers to cell proliferation in the calvaria. We have chosen to disregard this biological process since we believe its importance can be more accurately described in a future work where the effects of mechanical conditions, such as brain growth, in suture cells proliferation are considered. Hence, overall domain growth (skull growth) can be achieved following bone formation at the ossification fronts and sutures cell proliferation and matrix deposition influenced by mechanotransduction processes taking place in the underlying dura mater, caused by the growth of the brain.

1.7 Future Work

In order to validate the results obtained in the simulations, future experimental studies will be performed. A morphogenetic study on fetal mice will be made with the purpose of quantifying the expression of TGF-β2, TGF-β3, Wnt and Sclerostin along the calvaria during prenatal development till the beginning of weaning, usually at 21 days of life. Using immunostaining techniques, the expression of these molecules will be quantified and an assessment of their effects on bone formation and resorption processes will be carried out in the defined time frame. Additionally, TGF-β3 and Sclerostin knockout mice will be employed for assessing TGF-β3 and Sclerostin function on bone formation and resorption processes along the sutures.

1.8 Conclusion

The proposed biochemical model gives an initial approximation to the complex mechanisms that regulate the growth of the membranous bones of the skull and the formation, maintenance and interdigitation of the cranial sutures during human prenatal development and infancy. Unlike previous works, where sutures are studied after their formation, we describe how sutures form and maintain their phenotypical characteristics relying on complex biochemical regulatory mechanisms between osteoinhibitory and osteoinductive

molecules. These factors determine the time and location of suture formation during prenatal development and the emergence of the interdigitated patterns seen in sutures during infancy. The results of our model suggest that suture fate is dependent on the ability of suture cells to respond to biochemical signals coming from the developing flat bones by expressing osteoinhibitory proteins, suggesting that premature fusion of the sutures (also known as Craniosynostosis) might be the result of alterations in this sensory ability. Similarly, we show that interdigitated suture morphologies are the result of local variations in the concentration of biochemical factors along opposing bone fronts, which conjointly regulate bone formation and resorption events at the sutures. Therefore, this work provides a theoretical framework for the study of flat bone and suture morphogenesis, as well as pathologies related to it, such as Craniosynostosis, where abnormal bone formation along the sutures is present. This article could also give directions towards new types of experiments that help to understand the complex mechanobiological interactions present during calvarial development.

Appendix A. Estimation of the values of the parameters

The set of equations (1-12) correspond to a coupled reaction-diffusion system, similar to a Turing system that exhibits a diffusion-driven instability. For ($D_W, D_R \neq 0$), the distribution pattern will appear to some combination of parameters from the reactive and diffusive constants ($D_W, D_R, \nu, \gamma_0, \alpha_3, \alpha_4$) [76] that define the Turing space. To obtain the Turing space, a linear stability analysis about the steady state solution is needed [77], which is given by $\left(\frac{\partial S_W}{\partial t}\right)(D_W = 0) = 0$ and $\left(\frac{\partial R}{\partial t}\right)(D_R = 0) = 0$. This results in a steady state solution given by:

$$(S_W^*, S_R^*) = \frac{(\alpha_3 + \alpha_4)}{\nu}, \frac{\alpha_4 \nu^2}{\gamma_1(\alpha_4 + \alpha_4)^2} \tag{A1a}$$

where S_W^* and S_R^* are the steady-state values for the concentration of Wnt and Sclerostin, respectively. The linear analysis allows finding the range of parameters that ensure the emergence of such Turing patterns. Thus, the solution can be expressed as:

$$(S_W^*, S_R^*) = (\mu + S_W^*, \nu + S_R^*) \tag{A1b}$$

where μ and ν are small perturbations in each molecular factor, respectively. From Eqs. (A1a) and (A1b) and from the linear analysis (see [76]) we find the geometric area where the parameters of the reaction-diffusion equation are found, in such a way, to develop Turing patterns, this is

$$C_K(2\gamma_1 S_W^* S_R^* - \gamma_1 S_W^* - \nu) < 0 \tag{A2a}$$

$$C_K{}^2(\gamma_1(S_W^*)^2(\nu - 2\gamma_1 S_W^* S_R^*) + 2\gamma_1{}^2(S_W^*)^2 S_R^*) > 0 \quad \text{(A2b)}$$

$$C_K(D_R(2\gamma_1 S_W^* S_R^* - \nu) - D_W\gamma_1(S_R^*)^2) > 0 \quad \text{(A2c)}$$

$$C_K{}^2(D_R(2\gamma_1 S_W^* S_R^* - \nu) - D_W\gamma_1(S_W^*)^2)^2 - 4D_W D_R C_K{}^2(\gamma_1(S_W^*)^2(\nu - 2\gamma_1 S_W^* S_R^*) + 2\gamma_1{}^2(S_W^*)^2 S_R^*) > 0 \quad \text{(A2d)}$$

If we express Eqs. (1-12a) and (1-12b) into a non-dimensional form (Schnakenberg equation [76]) and as a function of small perturbations of the molecular factor (S_W, S_R), through (μ, ν) we can obtain:

$$\frac{\partial w}{\partial t} = \beta(c - w + w^2 x) + \nabla^2 w \quad \text{(A3a)}$$

$$\frac{\partial x}{\partial t} = \beta(d - w^2 x) + \mathrm{e}\nabla^2 x \quad \text{(A3b)}$$

where we can identify the parameters that move from the non-dimensional model (or Schnakenberg) to the real model given in Eq. (1-12) (see [77]). That is, we obtain the non-dimensionalization constants given by:

$$c = \frac{\alpha_3}{\nu}\sqrt{\frac{\gamma_1}{\nu}} \quad \text{(A4a)}$$

$$d = \frac{\alpha_4}{\nu}\sqrt{\frac{\gamma_1}{\nu}} \quad \text{(A4b)}$$

$$e = \frac{D_W}{D_R} \quad \text{(A4c)}$$

$$T = \frac{L^2}{D_R} \quad \text{(A4d)}$$

$$\beta = \frac{L^2}{D_R}\nu C_K \quad \text{(A4e)}$$

$$S_{W|REF} = S_{R|REF} = \sqrt{\frac{\nu}{\gamma_1}} \quad \text{(A4f)}$$

where T is the characteristic time of the processes of suture interdigitation and fusion during infancy (96 weeks) and L is the characteristic length of the bi-dimensional domain where these processes take place. Therefore, by defining (β, e, c, d), it is possible to obtain the eigenvalues and eigenvectors of the set of equations (Schnakenberg) and from them, the different spatial patterns corresponding to different wave numbers. **Table 1-1** shows the values of the constants from the non-dimensional model. In the case of the proposed dimensional model, it is necessary to define some parameters that are non-dimensional $(L, D_R, D_W, C_K, \nu, \gamma_1, \alpha_2, \alpha_3)$. The estimation of these values is made with the following recommendations:

1. The domain of study is a square of side 29 mm, given by a segment of the bone-suture-bone interface of the sagittal suture for a neonatal calvaria. The suture width is defined as 5 mm, based on findings from Mitchell et al. [55] regarding suture width for newborns at zero months of age. Then, the characteristic length is L=5 mm.
2. Hernandez et al. [78] found an average osteocyte count per bone area of $921\frac{cell}{mm^2}$ for woven bone formed via intramembranous ossification in the rat, when subjected to mechanical loading. Muller et al. [58] found an osteocyte density in trabecular bone of $10500\frac{cell}{mm^3}$ in humans.
3. This article has used average concentrations of $S_{W|REF}$ and $S_{R|REF}$ equal to $1\frac{ng}{ml}$.
4. Zhang et al. [59] found average concentrations of $10^{-6}\frac{cm^2}{s}$ for the diffusion coefficient of Wnt.

To reproduce the patterns of bone formation during suture interdigitation, it is necessary that all parameters are in the Turing space and therefore meet the restrictions (A2). Using (A4) we can find all the parameters that represent these biological processes, as seen in **Table 1-2**.

Table 1-2: Connection between the non-dimensional Schnakenberg model and the vibration modes according to the parameters obtained in the linear analysis.

e	$\boldsymbol{\beta}$	**c**	**d**
8.6076	535.0	0.1	0.9

References

[1] Shapiro RS, Robinson F. The embryogenesis of the human skull: An anatomic and radiographic atlas. Harvard University Press, Cambridge; 1980.

[2] Bronner F, Farch-Carson MC, Roach HI. Bone and development. 2010.

[3] Pattisapu JV, Gegg CA, Olavarria G, Johnson KK, Ruiz RL, Costello BJ. Craniosynostosis: diagnosis and surgical management. Atlas Oral Maxillofac Surg Clin North Am 2010;18:77–91. doi:10.1016/j.cxom.2010.08.002.

[4] Raam MS, Solomon BD, Shalev SA, Muenke M. Holoprosencephaly and Craniosynostosis: A Report of Two Siblings and Review of the Literature. Am J Med Genet 2010;154C:176–82. doi:10.1002/ajmg.c.30234.Holoprosencephaly.

[5] Ogle RC, Tholpady SS, McGlynn KA, Ogle RA. Regulation of cranial suture morphogenesis. Cells Tissues Organs 2004;176:54–66. doi:10.1159/000075027.

[6] Kiesler J, Ricer R. The Abnormal Fontanel. Am Fam Physician 2003;67:2547–52.

[7] Week 121: Skull, the temporal region n.d. http://www.dontbeasalmon.net/archives/2010/01/week-121-skull.html.

[8] Rice DP. Developmental anatomy of craniofacial sutures. Front Oral Biol 2008;12:1–21.

[9] Byron CD. Role of the osteoclast in cranial suture waveform patterning. Anat Rec A Discov Mol Cell Evol Biol 2006;288:552–63. doi:10.1002/ar.a.20322.

[10] Vu HL, Panchal J, Parker EE, Levine NS, Francel P. The timing of physiologic closure of the metopic suture: a review of 159 patients using reconstructed 3D CT scans of the craniofacial region. J Craniofac Surg 2001;12:527–32.

[11] Kumar V, Agarwal S, Bastia BK, MG S, Honnungar RS. Fusion of Skull Vault Sutures in Relation to Age-A Cross Sectional Postmortem Study Done in 3rd, 4th & 5th Decades of Life. J Forensic Res 2012;3:4–6. doi:10.4172/2157-7145.1000173.

[12] Alaqeel SM, Hinton RJ, Opperman LA. Cellular response to force application at craniofacial sutures. Orthod Craniofac Res 2006;9:111–22. doi:10.1111/j.1601-6343.2006.00371.x.

[13] Enlow DH. Normal craniofacial growth. Craniosynostosis diagnosis, Eval. Manag., 1986, p. 131–56.

[14] Greenwald JA, Mehrara BJ, Spector JA, Warren SM, Crisera FE, Fagenholz PJ, et al. Regional differentiation of cranial suture-associated dura mater in vivo and in vitro: implications for suture fusion and patency. J Bone Miner Res 2000;15:2413–30. doi:10.1359/jbmr.2000.15.12.2413.

[15] Herring SW. Mechanical Influences on Suture Development and Patency. Front Oral Biol 2008;12:41–56. doi:10.1159/0000115031.Mechanical.

[16] Herring SW, Teng S. Strain in the braincase and its sutures during function. Am J Phys Anthropol 2000;112:575–93.

[17] Opperman LA. Cranial Sutures as Intramembranous Bone Growth Sites. Dev Dyn 2000;219:472–85.

[18] Roth DA, Gold LI, Han VK, McCarthy JG, Sung JJ, Wisoff JH, et al. Immunolocalization of transforming growth factor beta 1, beta 2, and beta 3 and insulin-like growth factor I in premature cranial suture fusion. Plast Reconstr Surg 1997;99:300–9.

[19] Opperman LA, Moursi AM, Sayne JR, Wintergerst AM. Transforming growth factor-beta 3(Tgf-beta3) in a collagen gel delays fusion of the rat posterior interfrontal suture in vivo. Anat Rec 2002;267:120–30. doi:10.1002/ar.10094.

[20] Opperman LA, Chhabra A, Cho RW, Ogle RC. Cranial suture obliteration is induced by removal of transforming growth factor (TGF)-beta 3 activity and prevented by removal of TGF-beta 2 activity from fetal rat calvaria in vitro. J Craniofac Genet Dev Biol 1999;19:164–73.

[21] Opperman LA, Galanis V, Williams AR, Adab K. Transforming growth factor-beta3 (Tgf-beta3) down-regulates Tgf-beta3 receptor type I (Tbetar-I) during rescue of cranial sutures from osseous obliteration. Orthod Craniofacial Res 2002;5:5–16.

[22] Opperman LA, Adab K, Gakunga PT. Transforming growth factor-beta 2 and TGF-beta 3 regulate fetal rat cranial suture morphogenesis by regulating rates of cell proliferation and apoptosis. Dev Dyn 2000;219:237–47.

[23] Kramer I, Halleux C, Keller H, Pegurri M, Gooi JH, Weber PB, et al. Osteocyte Wnt/beta-catenin signaling is required for normal bone homeostasis. Mol Cell Biol 2010;30:3071–85. doi:10.1128/MCB.01428-09.

[24] Issack PS, Helfet DL, Lane JM. Role of wnt signaling in bone remodeling and repair. HSS J 2008;4:66–70. doi:10.1007/s11420-007-9072-1.

[25] Bonewald LF, Johnson ML. Osteocytes, Mechanosensing and Wnt Signaling. Bone 2008;42:606–15. doi:10.1016/j.biotechadv.2011.08.021.Secreted.

[26] Poole KE, Van Bezooijen RL, Loveridge N, Hamersma H, Papapoulos SE, Löwik CW, et al. Sclerostin is a delayed secreted product of osteocytes that inhibits bone formation. Fed Am Soc Exp Biol J 2005;19:1842–4.

[27] Lin C, Jiang X, Dai Z, Guo X, Weng T, Wang J, et al. Sclerostin mediates bone response to mechanical unloading through antagonizing Wnt/beta-catenin signaling. J Bone Miner Res 2009;24:1651–61.

[28] Ten D, Krause C, De Gorter DJ, Löwik CW, Van Bezooijen RL. Osteocyte-derived sclerostin inhibits bone formation: its role in bone morphogenetic protein and Wnt signaling. J Bone Jt Surg 2008;90:31–5.

[29] Beederman M, Farina EM, Reid RR. Molecular basis of cranial suture biology and disease: Osteoblastic and osteoclastic perspectives. Genes Dis 2014;1:120–5. doi:10.1016/j.gendis.2014.07.004.

[30] Karsenty G, Wagner EF. Reaching a genetic and molecular understanding of skeletal development. Dev Cell 2002;2:389–406. doi:10.1016/S1534-5807(02)00157-0.

[31] Glass DA, Bialek P, Ahn JD, Starbuck M, Patel M. S, Clevers H, et al. Canonical Wnt signaling in differentiated osteoblasts controls osteoclast differentiation. Dev Cell 2005;8:751–64. doi:10.1016/j.devcel.2005.02.017.

[32] Nakashima T, Hayashi M, Fukunaga T, Kurata K, Oh-Hora M, Feng JQ, et al. Evidence for osteocyte regulation of bone homeostasis through RANKL expression. Nat Med 2011;17:1231–4.

[33] Xiong J, O'Brien CA. Osteocyte RANKL: New insights into the control of bone remodeling. J Bone Miner Res 2012;27:499–505. doi:10.1002/jbmr.1547.

[34] Garzón-Alvarado DA, González A, Gutiérrez ML. Growth of the flat bones of the membranous neurocranium: a computational model. Comput Methods Programs Biomed 2013;112:655–64. doi:10.1016/j.cmpb.2013.07.027.

[35] Garzón-Alvarado DA. A hypothesis on the formation of the primary ossification centers in the membranous neurocranium: a mathematical and computational model. J Theor Biol 2013;317:366–76. doi:10.1016/j.jtbi.2012.09.015.

[36] Lee C, Richtsmeier JT, Kraft RH. A Computational Analysis of Bone Formation in the Cranial Vault in the Mouse. Front Bioeng Biotechnol 2015;3:1–11. doi:10.3389/fbioe.2015.00024.

[37] Khonsari RH, Olivier J, Vigneaux P, Sanchez S, Tafforeau P, Ahlberg PE, et al. A mathematical model for mechanotransduction at the early steps of suture formation. Proc Biol Sci 2013;280:20122670. doi:10.1098/rspb.2012.2670.

[38] Miura T, Perlyn CA, Kinboshi M, Ogihara N, Kobayashi-Miura M, Morriss-Kay GM, et al. Mechanism of skull suture maintenance and interdigitation. J Anat 2009;215:642–55. doi:10.1111/j.1469-7580.2009.01148.x.

[39] Zollikofer CPE, Weissmann JD. A bidirectional interface growth model for cranial interosseous suture morphogenesis. J Anat 2011;219:100–14. doi:10.1111/j.1469-7580.2011.01386.x.

[40] Garza RM, Khosla RK. Nonsyndromic craniosynostosis. Semin Plast Surg 2012;26:53–63. doi:10.1055/s-0032-1320063.

[41] Holleville N, Quilhac A, Bontoux M, Monsoro-Burq AH. BMP signals regulate Dlx5 during early avian skull development. Dev Biol 2003;257:177–89. doi:10.1016/S0012-1606(03)00059-9.

[42] Santos A, Bakker AD, Klein-Nulend J. The role of osteocytes in bone mechanotransduction. Osteoporos Int 2009;20:1027–31.

[43] Santos A, Bakker AD, Zandieh-Doulabi B, Semeins CM, Klein-Nulend J. Pulsating fluid flow modulates gene expression of proteins involved in Wnt signaling pathways in osteocytes. J Orthop Res 2009;27:1280–7. doi:10.1002/jor.20888.

[44] Ruch JV, Lesot H, Bègue-Kirn C. Odontoblast differentiation. Int J Dev Biol 1995;39:51–68.

[45] Schmitt R, Ruch JV. In vitro synchronization of embryonic mouse incisor preodontoblasts and preameloblasts: repercussions on terminal differentiation. Eur J Oral Sci 2000;108:311–9.

[46] Samee N, Geoffroy V, Marty C, Schiltz C, Vieux-Rochas M, Levi G, et al. Dlx5, a Positive Regulator of Osteoblastogenesis, is Essential for Osteoblast-Osteoclast Coupling. Am J Pathol 2008;173:773–80. doi:10.2353/ajpath.2008.080243.

[47] Chong SL, Mitchel LR, Moursi AM, Winnard P, Losken HW, Bradley J, et al. Rescue of coronal suture fusion using transforming growth factor-beta 3 (Tgf-beta 3) in rabbits with delayed-onset craniosynostosis. Anat Rec A Discov Mol Cell Evol Biol 2003;274:962–71.

[48] Delezoide AL, Benoist-Lasselin C, Legeai-Mallet L, Le Merrer M, Munnich A, Vekemans M, et al. Spatio-temporal expression of FGFR 1, 2 and 3 genes during human embryo-fetal ossification. Mech Dev 1998;77:19–30.

[49] Van Bezooijen RL, Svensson JP, Eefting D, Visser A, Van der Horst G, Karperien M, et al. Wnt but not BMP signaling is involved in the inhibitory action of sclerostin on BMP-stimulated bone formation. J Bone Miner Res 2007;22:19–28.

[50] Vanegas Acosta JC, Landinez Parra NS, Garzón-Alvarado DA. Implementación de modelos biológicos de reacción-difusión mediante el método de los elementos finitos. Rev Cuba Investig Biomédicas 2009;28.

[51] Wada T, Nakashima T, Hiroshi N, Penninger JM. RANKL-RANK signaling in osteoclastogenesis and bone disease. Trends Mol Med 2006;12:17–25. doi:10.1016/j.molmed.2005.11.007.

[52] Farley D, Dudley DJ. Fetal assessment during pregnancy. Pediatr Clin North Am 2009;56:489–504.

[53] Dennis JE, Merriam A, Awadallah A, Yoo JU, Johnstone B, Caplan AI. A quadripotential mesenchymal progenitor cell isolated from the marrow of an adult mouse. J Bone Miner Res 1999;14:700–9.

[54] Sadler TW. Langman's Medical Embriology. 9th ed. Baltimore, MD: Lippincott Williams and Wilkins; 2010.

[55] Mitchell LA, Kitley CA, Armitage TL, Krasnokutsky MV, Rooks VJ. Normal sagittal and coronal suture widths by using CT imaging. Am J Neuroradiol 2011;32:1801–5. doi:10.3174/ajnr.A2673.

[56] Vandyke H. Anatomy of the Human Body. 1918.

[57] Albro MB, Nims RJ, Cigan AD, Yeroushalmi KJ, Alliston T, Hung CT, et al. Accumulation of Exogenous Activated TGF-β in the Superficial Zone of Articular Cartilage. Biophys J 2013;104:1794–804. doi:10.1016/j.bpj.2013.02.052.

[58] Mullender MG, Van Der Meer DD, Huiskes R, Lips P. Osteocyte density changes in aging and osteoporosis. Bone 1996;18:109–13. doi:10.1016/8756-3282(95)00444-0.

[59] Zhang L, Lander AD, Nie Q. A reaction–diffusion mechanism influences cell lineage progression as a basis for formation, regeneration, and stability of intestinal crypts. BMC Syst Biol 2012;6:93. doi:10.1186/1752-0509-6-93.

[60] Behr B, Longaker MT, Quarto N. Differential activation of canonical Wnt signaling determines cranial sutures fate: a novel mechanism for sagittal suture craniosynostosis. Dev Biol 2010;344:922–40. doi:10.1016/j.ydbio.2010.06.009.

[61] Coussens AK, Hughes IP, Wilkinson CR, Morris CP, Anderson PJ, Powell BC, et al. Identification of genes differentially expressed by prematurely fused human sutures using a novel in vivo - in vitro approach. Differentiation 2008;76:531–45. doi:10.1111/j.1432-0436.2007.00244.x.

[62] Dwivedi PP, Grose RH, Filmus J, Hii CST, Xian CJ, Anderson PJ, et al. Regulation of bone morphogenetic protein signalling and cranial osteogenesis by Gpc1 and Gpc3. Bone 2013;55:367–76. doi:10.1016/j.bone.2013.04.013.

[63] Oppenheimer AJ, Rhee ST, Goldstein SA, Buchman SR. Force-Induced Craniosynostosis in the Murine Sagittal Suture. Plast Reconstr Surg 2009;124:1840–8. doi:10.1097/PRS.0b013e3181bf806c.Force-Induced.

[64] Opperman LA, Passarelli RW, Nolen AA, Gampper TJ, Lin KYK, Ogle RC. Dura mater secretes soluble heparing-binding factors required for cranial suture morphogenesis. Vitr Cell Dev Biol - Anim 1996;32:627–32.

[65] Opperman LA, Sweeney TM, Redmon J, Persing JA, Ogle RC. Tissue interactions with underlying dura mater inhibit osseous obliteration of developing cranial sutures. Dev Dyn 1993;198:312–22.

[66] Opperman LA, Passarelli RW, Morgan EP, Reintjes M, Ogle RC. Cranial sutures require tissue interactions with dura mater to resist osseous obliteration in vitro. J Bone Miner Res 1995;10:1978–87.

[67] Cohen MMJ. Sutural biology and the correlates of craniosynostosis. Am J Med Genet 1993;47:581–616.

[68] Opperman LA, Nolen AA, Ogle RC. TGF-β1, TGF-β2, and TGF-β3 Exhibit Distinct Patterns of Expression During Cranial Suture Formation and Obliteration In Vivo and In Vitro. J Bone Miner Res 1997;12:301–10.

[69] Holmes G, Rothschild G, Roy UB, Deng CX, Mansukhani A, Basilico C. Early onset of craniosynostosis in an Apert mouse model reveals critical features of this pathology. Dev Biol 2009;328:273–84. doi:10.1016/j.ydbio.2009.01.026.

[70] Bowling EL, Burstein FD. Crouzon syndrome. Optometry 2006;77:217–22. doi:10.1016/j.optm.2006.03.005.

[71] Nur BG, Pehlivanoğlu S, Mıhçı E, Calışkan M, Demir D, Alper OM, et al. Clinicogenetic study of Turkish patients with syndromic craniosynostosis and literature review. Pediatr Neurol 2014;50:482–90. doi:10.1016/j.pediatrneurol.2014.01.023.

[72] Markey MJ, Main RP, Marshall CR. In vivo cranial suture function and suture morphology in the extant fish Polypterus: implications for inferring skull function in living and fossil fish. J Exp Biol 2006;209:2085–102. doi:10.1242/jeb.02266.

[73] Sun Z, Lee E, Herring SW. Cranial Sutures and Bones: Growth and Fusion in Relation to Masticatory Strain. Anat Rec 2004;276:150.

doi:10.1002/ar.a.20002.Cranial.

[74] Rafferty KL, Herring SW. Craniofacial Sutures: Morphology, Growth, and In Vivo Masticatory Strains. J Morphol 1999;242:167–79. doi:10.1002/(SICI)1097-4687(199911)242.

[75] Herring SW, Teng S. Strain in the Braincase and Its Sutures During Function. Am J Phys Anthropol 2000;112:575–93. doi:10.1002/1096-8644(200008)112.

[76] Garzon-Alvarado DA, Ramirez Martinez AM. A biochemical hypothesis on the formation of fingerprints using a turing patterns approach. Theor Biol Med Model 2011;8.

[77] Garzón-Alvarado DA, Galeano CH, Mantilla JM. Turing pattern formation for reaction–convection–diffusion systems in fixed domains submitted to toroidal velocity fields. Appl Math Model 2011;35:4913–25. doi:10.1016/j.apm.2011.03.040.

[78] Hernandez CJ, Majeska RJ, Schaffler MB. Osteocyte density in woven bone. Bone 2004;35:1095–9.